# Phonon dispersion curves and atomic mean square displacement for several fcc and bcc materials

by

C. Robert Pinnegar, B.Sc.

A Thesis

submitted to the Department of Physics

in partial fulfillment of the requirements

for the degree of

Master of Science

December 1995

Brock University

St.Catharines, Ontario

## Table of Contents

# Abstract

The atomic mean square displacement (MSD) and the phonon dispersion curves (PDC's) of a number of face-centred cubic (fcc) and body-centred cubic (bcc) materials have been calculated from the quasiharmonic (QH) theory, the lowest order ($\lambda^2$) perturbation theory (PT) and a recently proposed Green's function (GF) method by Shukla and Hübschle. The latter method includes certain anharmonic effects to all orders of anharmonicity.

In order to determine the effect of the range of the interatomic interaction upon the anharmonic contributions to the MSD we have carried out our calculations for a Lennard-Jones (L-J) solid in the nearest-neighbour (NN) and next-nearest neighbour (NNN) approximations. These results can be presented in dimensionless units but if the NN and NNN results are to be compared with each other they must be converted to that of a real solid. When this is done for Xe, the QH MSD for the NN and NNN approximations are found to differ from each other by about 2%. For the $\lambda^2$ and GF results this difference amounts to 8% and 7% respectively. For the NN case we have also compared our PT results, which have been calculated exactly, with PT results calculated using a frequency-shift approximation. We conclude that

this frequency-shift approximation is a poor approximation.

We have calculated the MSD of five alkali metals, five bcc transition metals and seven fcc transition metals. The model potentials we have used include the Morse, modified Morse, and Rydberg potentials. In general the results obtained from the Green's function method are in the best agreement with experiment. However, this improvement is mostly qualitative and the values of MSD calculated from the Green's function method are not in much better agreement with the experimental data than those calculated from the QH theory.

We have calculated the phonon dispersion curves (PDC's) of Na and Cu, using the 4 parameter modified Morse potential. In the case of Na, our results for the PDC's are in poor agreement with experiment. In the case of Cu, the agreement between the theory and experiment is much better and in addition the results for the PDC's calculated from the GF method are in better agreement with experiment that those obtained from the QH theory.

# Acknowledgements

It is a pleasure to thank Dr. R.C.Shukla for suggesting this project, for his invaluable assistance and helpful suggestions throughout the course of its evolution, and for his financial assistance through his NSERC grant.

I would also like to thank my parents for their love and their support (both financial and moral). I love you both.

## List of Tables

## List of Figures

# 1. Introduction

The objective in this thesis is to report the results of our calculations of the mean-square atomic displacement (MSD) and phonon dispersion curves (PDC's) of a number of monatomic face-centred cubic (fcc) and body-centred cubic (bcc) materials. In these calculations we have included the quasiharmonic and the lowest order cubic and quartic anharmonic contributions to the MSD. Since results for MSD, calculated in the harmonic approximation from a wide variety of models, are available in the existing literature, we first provide a short review of these models and point out their shortcomings as well as the deficiencies in the numerical procedures used in their calculation. Next we summarize what is known of the anharmonic calculation of the MSD. We then briefly summarize the results of calculations of the MSD for different classes of solids which have been performed using the quasiharmonic and anharmonic theory and the Green's function method proposed by Shukla and Hübschle (1989a). Finally we briefly describe what is experimentally known of the phonon dispersion curves of the two metals for which our calculations have been carried out.

Due to the thermal motions of atoms, the intensity of a scattered beam

of X-rays or neutrons is reduced by a temperature-dependent exponential factor given by

$$I(T) = I_0 \, exp(-2W)$$

where $I_0$ is the intensity at absolute zero and $I(T)$ is the intensity at temperature $T$. $2W$ is the Debye-Waller factor which is proportional to the MSD. Among the three states of matter, solid, liquid and gas, crystalline solids are very special because the translational and rotational symmetries which they possess provide a considerable reduction in the mathematics of the formalism needed in the calculation of the MSD and of other thermodynamic properties.

Most calculations of the MSD have been carried out in the harmonic approximation, in which the Taylor series expansion of the crystal potential about its equilibrium configuration is truncated after the quadratic term. A wide variety of models have been used in these harmonic calculations, some of which have theoretical shortcomings; for example, any model whose formalism violates the translational and rotational symmetry of the crystal lattice (Pal 1973; Kharoo et al. 1977) cannot be physically valid. The

functional form for MSD is very sensitive to the number of points $N$ employed in its numerical evaluation because the contribution from the long wavelength region is weighted heavily. If the MSD is calculated using several different finite values of $N$ an extrapolation to $N \rightarrow \infty$ can be performed which provides an exact answer to the sum (Heiser, Shukla and Cowley 1986). In the vast majority of harmonic calculations in the existing literature (for example Tripathi and Behari 1971; Prakash, Pathak and Hemkar 1975; Gupta 1975; Prakash and Hemkar 1973; Kushwawa 1979; Sangal and Sharma 1971) this extrapolation method has not been included in the evaluation of the MSD.

At low temperatures the harmonic approximation is usually adequate in predicting the MSD and thermodynamic properties of a solid. At higher temperatures the role of the omitted higher-order terms in the Taylor series expansion of the crystal potential energy becomes important and these terms have to be considered in the calculation of the MSD and the thermodynamic properties of the system. These are the anharmonic terms of the Hamiltonian and the phenomena they give rise to are referred to as anharmonic effects. Several important properties of bulk solids fall into this category, including the thermal expansion of solids, the temperature dependence of thermal resistivity, and the deviation of the specific heat from the classical Dulong-Petit

law at high temperature. The harmonic approximation can explain none of these phenomena.

The implicit anharmonic contribution to all thermodynamic and MSD calculations can be included by performing harmonic calculations at different volumes and allowing the phonon frequencies to vary continuously with the volume of the crystal. This is known as the quasiharmonic (QH) approximation. However for the evaluation of the full anharmonic contribution the explicit anharmonic terms have to be included in addition to the QH contribution.

The explicit anharmonic contributions can be calculated by a variety of methods. The most commonly used is perturbation theory (PT) in which the QH approximation is used to describe the unperturbed state and the anharmonic contributions to the MSD and thermodynamic properties are expressed in terms of the QH eigenvalues and eigenvectors of the system and of the Cartesian derivatives of the potential function.

In PT we want to group together terms which are of the same order of anharmonicity. This is accomplished via the introduction of an ordering parameter such as the Van Hove ordering parameter $\lambda$, which is defined to be the square root of the MSD divided by the interatomic nearest neighbour dis-

tance. All terms in the perturbation expansion of the MSD can be grouped by order in $\lambda$. The first term in the expansion is the QH contribution which is of order $\lambda^0$. By symmetry all terms of odd order in $\lambda$ vanish. The next two non-zero terms, the cubic and quartic, are of order $\lambda^2$. These two terms are of similar magnitude but are of opposite sign, so both must be included in the $\lambda^2$ PT result. Inclusion of one without the other can lead to serious errors in numerical results (Shukla 1994). The classical (or high-temperature) expressions for the cubic and quartic anharmonic contributions to MSD were first derived by Maradudin and Flinn (1963) who evaluated them approximately for a nearest neighbour (NN) central force model of a fcc crystal in the leading-term approximation (LTA). Shukla and Plint (1989) (SP) however have found that the $\lambda^2$ anharmonic contribution to MSD obtained from the LTA has the wrong sign. Therefore the LTA has not been used in any of our calculations.

The MSD of a NN central force fcc solid has been calculated, in the QH approximation and to order $\lambda^2$ exactly, by Heiser, Shukla and Cowley (1986) (HSC) for the Lennard-Jones (L-J) potential. In the absence of experimental

values of MSD for a L-J solid, HSC compared their $\lambda^2$ PT results with results obtained from the Monte Carlo (MC) method which was also used by these authors in the computation of MSD. In some sense the MC results are the data obtained from the computer experiment. The comparison of the $\lambda^2$ and MC results revealed that the $\lambda^2$ theory was adequate up to $\frac{3}{4}T_m$ where $T_m$ is the melting temperature of the solid.

To overcome the inadequacy of the $\lambda^2$ PT a Green's function method has been proposed by Shukla and Hübschle (1989a)(SH1). They used the Green's function method to calculate the MSD of a NN L-J fcc solid, and compared their results with HSC. At all temperatures the values of MSD obtained from the Green's function method were found to be in better agreement with the MC results than the values of MSD obtained using $\lambda^2$PT. The agreement between the Green's function and MC results was excellent except near the melting point where the Green's function results were about 6% lower than the MC results.

The only other fcc system for which a similar type of extensive investigation of MSD has been carried out is Al. The MSD of Al has been calculated, in the QH approximation and using $\lambda^2$PT, by SP. In their calculations SP used two forms of the Morse potential. The first of these was the familiar

3 parameter Morse potential and the second was a 4 parameter modified Morse potential. For both potential functions the calculations of MSD were performed in the NN approximation. The results from the modified Morse potential were found to be in better agreement with experimental data than the results obtained from the 3 parameter Morse potential.

The Green's function method was first used to calculate the MSD of Al by Shukla and Hübschle (1989b) (SH2). Their results, obtained using the 3 parameter Morse potential, were in poor agreement with experiment. Since the 4 parameter modified Morse potential was not used by SH2 in their calculations, it would be interesting (in light of the results of SP) to use the Green's function method to calculate the MSD of Al using the 4 parameter modified Morse potential, and to determine whether the results are in better agreement with experiment than those calculated from the 3 parameter Morse potential. The comparison of results for MSD obtained from the 3 parameter Morse potential and the 4 parameter modified Morse potential can also be carried out for several other fcc metals for which the parameters of these potentials are known (Macdonald and Macdonald 1981).

The MSD of the alkali metals was calculated for the first time, in the QH approximation and using $\lambda^2$ PT and molecular-dynamics (MD) simulations, by Shukla and Mountain (1982) (SM1) and Shukla and Heiser (1986) (SH3). They used a sixth-neighbour interaction obtained from the Ashcroft pseudopotential and Vashishta-Singwi screening function (AVS). Here the MD results (again a kind of computer experiment) replace the real experimental data. Good agreement was found between the MD and $\lambda^2$ PT results at temperatures up to $T_m$ except in the case of Cs where the difference was found to be about 15% near $T_m$.

Hübschle and Shukla (1989) (HS) used the QH theory, $\lambda^2$ PT and the Green's function method to calculate the MSD of Na, K and Cs. HS used the same pseudopotential function, potential parameters and lattice constants which had previously been used in SH3. HS found that near $T_m$ the values of MSD calculated from the Green's function method were only about 3% higher than the corresponding results obtained using $\lambda^2$ PT and were not in much better agreement with the MD results of SH3 than the $\lambda^2$ PT results.

Since Green's function calculations of the MSD of the bcc alkali metals have not been done using a potential function other than the AVS pseudopotential, it would be of interest to use the Green's function method to

calculate the MSD of bcc alkali metals using a potential function such as the Morse potential or the Rydberg potential, and to compare the values of MSD obtained from those calculations with experimental values of MSD. Since the Morse and Rydberg potential parameters are also available for several bcc transition metals (Macdonald and Shukla 1985) the MSD of these metals can also be determined using the QH, $\lambda^2$ PT and Green's function methods.

Unlike the fcc case, for bcc materials it is essential to include both the nearest- and next-nearest neighbour interactions in the harmonic and anharmonic calculation of MSD. It has been demonstrated (Shukla 1981) that in the calculation of anharmonic effects in bcc metals the NN approximation produces misleading results. This problem arises because the nearest- and next-nearest neighbour distances are almost equal in the bcc lattice and therefore the interaction range of the pair potential must include the second neighbour shell. This is the next-nearest neighbour (NNN) approximation. For fcc solids, the Green's function method has not been used to calculate the MSD in the NNN approximation and it would be of interest to carry out these calculations using the QH, $\lambda^2$ PT and Green's function methods and to compare our results with the NN results in order to determine whether the second-neighbour interactions affect the values of MSD.

The phonon dispersion curves of a solid (Al) were first obtained experimentally by Olmer (1948) using thermal diffuse scattering of X-rays (TDS). Subsequently TDS was used by Jacobsen (1955) to measure the PDC's of Cu. The TDS method was eventually superseded by the more accurate technique of inelastic neutron scattering (INS), first used by Brockhouse and Stewart (1955) to measure the PDC's of Al.

The INS method was first applied to Cu by Cribier et al. (1961). Their initial work has since been improved upon by the more detailed results of Sinha (1966), Svensson et al. (1967), Nicklow et al. (1967), and Miller and Brockhouse (1971). Larose and Brockhouse (1976) obtained the PDC's of Cu for the first time at $T \sim T_m$. INS has also been used to obtain the PDC's of other solids. The measurements for Na were performed for the first time by Woods et al. (1962) and later by Millington and Squires (1971). The latter results were obtained at $T \sim T_m$.

Since the anharmonicity is largest around $T = T_m$ the contribution of anharmonic effects to the phonon frequencies can be calculated through the Green's function method. Such frequencies are known as the renormalized phonon frequencies and indeed they are the ones which should be compared with the real experimental data of Cu and Na at $T \sim T_m$.

The outline of this thesis is as follows: In Chapter 2 we provide a summary of some theoretical results of the Green's function method which are relevant to the calculation of the MSD and PDC's of solids. We also describe the numerical procedures used in these Green's function calculations, and in similar calculations which were carried out in the QH approximation and using $\lambda^2$ PT.

In Chapter 3 we report the results of our calculations of MSD for a Lennard-Jones solid (Xe) which were carried out in the NN and NNN approximations in order to determine whether the second neighbour interactions are important in the calculation of MSD. We also compare our $\lambda^2$ PT results for the MSD of Xe with those of Goldman (1968) which were obtained using a frequency-shift approximation. Since our calculations have been done exactly this comparison will determine whether the frequency-shift approximation is valid.

We then report the results of our calculations of MSD for seven fcc metals, five bcc alkali metals, and five bcc transition metals. For each class of substance the model potentials used in our numerical procedure are also described. Wherever possible our results for MSD are compared with experimental data and (for K alone) with the results of the calculations of SH1

which were obtained from the AVS pseudopotential.

In Chapter 4 we report the results of our calculation of the phonon dispersion curves of Na and Cu. These have been obtained using the QH and Green's function methods. Our results are compared with experimental data.

A summary of our results is presented in Chapter 5.

# 2. Calculation of MSD

In this chapter we describe the theory and numerical procedures which we have used in our calculation of the MSD and PDC's of fcc and bcc solids. We begin by briefly summarizing the theory of the calculation of MSD.

Next we present (without outlining the whole theory) the Green's function method of Shukla and Hübschle from which we have obtained the MSD and PDC's of a number of cubic solids in the high-temperature limit and in the static approximation (to be discussed later).

Finally we summarize the numerical procedure required in the calculation of MSD using the Green's function method. The numerical procedures required in the calculation of MSD in the QH approximation and using $\lambda^2$ PT are also briefly described since we have also used these methods to calculate the MSD of solids for the purpose of comparison with the results obtained from the Green's function method.

## 2.1. Mean Square Displacement

The instantaneous displacement of an atom from its equilibrium position in the crystal lattice can be expressed in terms of a superposition of all the normal vibrational modes of the crystal. In a regular periodic crystal the

normal modes are plane waves and their quantized states are called *phonons.* The Fourier expansion of the atomic displacement involves the harmonic eigenvalues (or frequencies) $\omega(\mathbf{q}j)$ and the eigenvectors $\mathbf{e}(\mathbf{q}j)$ and wavevectors $\mathbf{q}$ of all the phonon modes of the system. In second quantized form the plane-wave representation of the displacement is (Shukla and Hübschle 1989a):

$$u_\alpha^\ell(t) = \left[\frac{\hbar}{2NM}\right]^{1/2} \sum_{\mathbf{q}j} \frac{e_\alpha(\mathbf{q}j)}{(\omega(\mathbf{q}j))^{1/2}} exp[i\mathbf{q}\cdot\mathbf{r}_\ell] A_{\mathbf{q}j}(t) \qquad (1)$$

In Eq.( 1), $u_\alpha^\ell(t)$ is the instantaneous displacement of the $\ell^{th}$ atom in the crystal from its equilibrium position, in the $\alpha$-Cartesian direction, at time $t$. $\hbar$ is Planck's constant divided by $2\pi$. $N$ is the number of unit cells in the crystal, $M$ is the atomic mass, and $e_\alpha(\mathbf{q}j)$ is the $\alpha$-Cartesian component of $\mathbf{e}(\mathbf{q}j)$. $\mathbf{r}_\ell$ is the position vector of the $\ell^{th}$ lattice point. The quantity $j$ denotes the branch index of a phonon mode. Hereafter the phonon mode having wavevector $\mathbf{q}$ and branch index $j$ will be referred to as the $\mathbf{q}j^{th}$ phonon mode. The sum over $\mathbf{q}$ includes all the phonon wavevectors within the first Brillouin zone (FBZ) of the crystal. We have used the notation

$$A_{\mathbf{q}j} = a_{\mathbf{q}j} + a^{\dagger}_{-\mathbf{q}j} \tag{2}$$

where $a^{\dagger}_{\mathbf{q}j}$ and $a_{\mathbf{q}j}$ are the usual phonon creation and annihilation operators. The time dependence of $A_{\mathbf{q}j}$ is in the Heisenberg representation. $H$ denotes the Hamiltonian of the system. The expression for MSD is obtained by squaring Eq.( 1) and taking the thermal average:

$$< u^2 >= \frac{\hbar}{2NM} \sum_{\alpha} \sum_{\mathbf{q}_1 j_1 \mathbf{q}_2 j_2} \frac{e_\alpha(\mathbf{q}_1 j_1) e_\alpha(\mathbf{q}_2 j_2)}{[\omega(\mathbf{q}_1 j_1)\omega(\mathbf{q}_2 j_2)]^{(1/2)}} exp[i(\mathbf{q}_1 - \mathbf{q}_2)\cdot\mathbf{r}_\ell] < A_{\mathbf{q}_1 j_1}{}^{\dagger} A_{\mathbf{q}_2 j_2} > \tag{3}$$

The angular brackets denote the thermal average. For an operator $O$, this is defined by:

$$< O >= \frac{Tr(Oe^{-\beta H})}{Tr(e^{-\beta H})} \tag{4}$$

Here $\beta = 1/k_B T$ where $k_B$ is the Boltzmann constant and $T$ is the temperature. In order to obtain the MSD for a given Hamiltonian we must therefore evaluate the quantity $< A_{\mathbf{q}_1 j_1}{}^{\dagger} A_{\mathbf{q}_2 j_2} >$ in Eq.( 3).

## 2.2. The Green's function method

In the harmonic approximation, the Taylor series expansion of the crystal potential energy is truncated after the quadratic term. In PT of lowest order, and in the Green's function method of Shukla and Hübschle, the cubic and quartic terms in the Taylor expansion are also included in the Hamiltonian of the system, which is expressed as the sum of the harmonic component $H_0$ and an anharmonic component $H'$:

$$H = H_0 + H' \tag{5}$$

$$H_0 = \sum_{\mathbf{q}j} \hbar\omega(\mathbf{q}j)(a^{\dagger}_{\mathbf{q}j} a_{\mathbf{q}j} + \frac{1}{2}), \tag{6}$$

$$\begin{aligned} H' = \quad & \lambda \sum_{\mathbf{q}_1 j_1, \mathbf{q}_2 j_2, \mathbf{q}_3 j_3} V^3(\mathbf{q}_1 j_1, \mathbf{q}_2 j_2, \mathbf{q}_3 j_3) A_{\mathbf{q}_1 j_1} A_{\mathbf{q}_2 j_2} A_{\mathbf{q}_3 j_3} + \\ & \lambda^2 \sum_{\mathbf{q}_1 j_1, \mathbf{q}_2 j_2, \mathbf{q}_3 j_3, \mathbf{q}_4 j_4} V^4(\mathbf{q}_1 j_1, \mathbf{q}_2 j_2, \mathbf{q}_3 j_3, \mathbf{q}_4 j_4) A_{\mathbf{q}_1 j_1} A_{\mathbf{q}_2 j_2} A_{\mathbf{q}_3 j_3} A_{\mathbf{q}_4 j_4} \end{aligned} \tag{7}$$

In Eq.( 7), $\lambda$ is the Van Hove ordering parameter and $V^3$ and $V^4$ are the Fourier transforms of the third and fourth order atomic force constants. These are defined by (Shukla and Wilk 1974):

$$V^n(\mathbf{q}_1 j_1, \ldots, \mathbf{q}_n j_n) = \frac{N^{1-n/2}}{n!}\left(\frac{\hbar}{2}\right)^n \Delta(\mathbf{q}_1 + \cdots + \mathbf{q}_n)\frac{\Phi^n(\mathbf{q}_1 j_1, \ldots, \mathbf{q}_n j_n)}{(\omega(\mathbf{q}_1 j_1)\cdots\omega(\mathbf{q}_n j_n))^{1/2}} \quad (8)$$

$$\Phi^n(\mathbf{q}_1 j_1, \ldots, \mathbf{q}_n j_n) = \frac{1}{2M^{n/2}}{\sum_{\ell_1}}' \sum_{\alpha,\ldots,\delta} \phi_{\alpha,\ldots,\delta}(\ell_1) e_\alpha(\mathbf{q}_1 j_1)\cdots e_\delta(\mathbf{q}_n j_n) \quad (9)$$
$$\times(1 - e^{-i\mathbf{q}_1\cdot\mathbf{r}_{\ell_1}}) \times \cdots \times (1 - e^{i\mathbf{q}_n\cdot\mathbf{r}_{\ell_1}})$$

In Eq.( 9) $\phi_{\alpha,\ldots,\delta}(\ell_1)$ is the Cartesian tensor derivative of the potential function at the $\ell_1^{th}$ lattice point. The method by which these tensor derivatives are obtained has been described thoroughly by Shukla and Plint (1989) so we will not repeat it here. The $\Delta(\mathbf{q})$ function is equal to 1 if its argument is zero or a reciprocal lattice vector, and is equal to zero otherwise.

The derivation of the Green's function method is very lengthy and has been outlined in detail elsewhere (Zubarev 1960; Shukla and Muller 1971; Shukla and Hübschle 1989a) so we will only summarize some previously reported results of this derivation which are relevant to our calculation of the MSD and PDC's of solids.

Shukla and Muller (1971) have obtained the expression for the double-time temperature-dependent Green's function $G^{jj'}_{\mathbf{q}\mathbf{q}'}(t)$ for the anharmonic Hamiltonian of Eq.( 5). The Fourier transform of this is expressed as

$$G^{jj'}_{\mathbf{q}\mathbf{q}'}(\omega) = \frac{\omega(\mathbf{q}j)\delta_{\mathbf{q}\mathbf{q}'}\delta_{jj'}}{\pi[\omega^2 - \omega^2(\mathbf{q}j) - 2\omega(\mathbf{q}j)\Pi_{\mathbf{q}j}(\omega)]} \tag{10}$$

In Eqs.( 10) and ( 11), $\delta_{\mathbf{q}\mathbf{q}'}$ and $\delta_{jj'}$ are Kronecker delta functions. $\Pi_{\mathbf{q}j}(\omega)$ is known as the phonon self-energy term. $\Pi_{\mathbf{q}j}(\omega)$ contains quartic and cubic components. The quartic component is independent of $\omega$ but the cubic component has $\omega$-dependence. If this $\omega$-dependence is assumed to be weak and the cubic component of $\Pi_{\mathbf{q}j}(\omega)$ is evaluated for $\omega = 0$ (static approximation), $G^{jj'}_{\mathbf{q}\mathbf{q}'}(\omega)$ then reduces to the following simple form:

$$G^{jj'}_{\mathbf{q}\mathbf{q}'}(\omega) = \frac{\omega(\mathbf{q}j)\delta_{\mathbf{q}\mathbf{q}'}\delta_{jj'}}{\pi[\omega^2 - \Omega^2(\mathbf{q}j)(\omega = 0)]} \tag{11}$$

The quantity $\Omega(\mathbf{q}j)$ is the renormalized (or RE) phonon frequency. In the high-temperature limit ($T > \Theta$, where $\Theta$ is the Debye temperature of the solid) $\Omega(\mathbf{q}j)$ is expressed as (Shukla and Hübschle 1989a):

$$\begin{aligned}\Omega^2(\mathbf{q}j) = \omega^2(\mathbf{q}j) \quad & -\tfrac{\lambda^2 k_B T}{2N} \sum_{\mathbf{q}_1 j_1 \mathbf{q}_2 j_2} \Delta(\mathbf{q}_1 + \mathbf{q}_2 - \mathbf{q}) \frac{|\Phi^3(\mathbf{q}_1 j_1, \mathbf{q}_2 j_2, -\mathbf{q}j)|^2}{\omega^2(\mathbf{q}_1 j_1)\omega^2(\mathbf{q}_2 j_2)} \\ & + \tfrac{\lambda^2 k_B T}{2N} \sum_{\mathbf{q}_1 j_1} \frac{\Phi^4(\mathbf{q}_1 j_1, -\mathbf{q}_1 j_1; \mathbf{q}_2 j_2, -\mathbf{q}_2 j_2)}{\omega^2(\mathbf{q}_1 j_1)}\end{aligned} \tag{12}$$

$$\text{or}, \Omega^2(\mathbf{q}j) = \omega^2(\mathbf{q}j) + \Delta_3(\mathbf{q}j) + \Delta_4(\mathbf{q}j) \tag{13}$$

Here the quantities $\Delta_3(\mathbf{q}j)$ and $\Delta_4(\mathbf{q}j)$ are cubic and quartic anharmonic phonon frequency shifts. These are due to the corresponding anharmonic terms in the Hamiltonian. From Eq.( 11) the quantity $< A_{\mathbf{q}_1 j_1}{}^{\dagger} A_{\mathbf{q}_2 j_2} >$ in Eq.( 3) is obtained, yielding the high-temperature RE expression for MSD:

$$< u^2 >_{RE} = \frac{k_B T}{NM} \sum_{\mathbf{q}j} \frac{1}{\Omega^2(\mathbf{q}j)} \tag{14}$$

Substitution of the expression for $\Omega(\mathbf{q}j)$ in Eq.( 12) into Eq.( 14) and expansion of the RHS in a binomial expansion in powers of $\lambda$, yields three terms to $O(\lambda^2)$:

$$< u^2 >_{QH} = \frac{k_B T}{NM} \sum_{\mathbf{q}j} \frac{1}{\omega^2(\mathbf{q}j)} \tag{15}$$

$$< u^2 >_{Q} = -\frac{(k_B T)^2 \lambda^2}{2N^2 M} \sum_{\mathbf{q}_1 j_1 \mathbf{q}_2 j_2} \frac{\Phi^4(\mathbf{q}_1 j_1, -\mathbf{q}_1 j_1; \mathbf{q}_2 j_2, -\mathbf{q}_2 j_2)}{\omega^2(\mathbf{q}_1 j_1)\omega^4(\mathbf{q}_2 j_2)} \tag{16}$$

$$< u^2 >_{C} = \frac{(k_B T)^2 \lambda^2}{2N^2 M} \sum_{\mathbf{q}_1 j_1 \mathbf{q}_2 j_2 \mathbf{q}_3 j_3} \Delta(\mathbf{q}_1 + \mathbf{q}_2 + \mathbf{q}_3) \frac{|\Phi^3(\mathbf{q}_1 j_1; \mathbf{q}_2 j_2; \mathbf{q}_3 j_3)|^2}{\omega^2(\mathbf{q}_1 j_1)\omega^2(\mathbf{q}_2 j_2)\omega^4(\mathbf{q}_3 j_3)} \tag{17}$$

The expressions for $< u^2 >_{QH}$, $< u^2 >_{Q}$ and $< u^2 >_{C}$ in Eqs.( 15), ( 16) and ( 17) are, respectively, the same as the high-temperature expressions for

the harmonic, quartic and cubic anharmonic contributions to MSD which are obtained using $\lambda^2$ PT (Shukla and Hübschle 1989a). This demonstrates that in this order of $\lambda$ the static approximation produces exact results. The $\lambda^2$ PT expression for $< u^2 >$ is the sum of these three terms:

$$< u^2 >_{PT} = < u^2 >_{QH} + < u^2 >_Q + < u^2 >_C \qquad (18)$$

The Green's function result for MSD however also includes anharmonic contributions which are of order higher than $\lambda^2$. In this thesis the numerical difference between $< u^2 >_{RE}$ and $< u^2 >_{QH}$ will be referred to as the RE anharmonic contribution to MSD and the sum of $< u^2 >_Q$ and $< u^2 >_C$ will be referred to as the $\lambda^2$ anharmonic contribution to MSD. This should not be confused with the $\lambda^2$ PT *result* which is expressed by $< u^2 >_{PT}$ in Eq.( 18).

In Eqs.( 15), ( 16) and ( 17) the subscript QH denotes the quasiharmonic approximation, in which the formalism is the same as in the harmonic case but in which the $\omega(\mathbf{q}j)$ are permitted to vary continuously with the volume of the crystal in order to account for the effects of thermal lattice expansion. In all our calculations of the MSD and phonon frequencies of solids, $\omega(\mathbf{q}j)$ denotes a QH frequency.

In addition to providing us with the information needed to evaluate the MSD, the knowledge of the $\omega(\mathbf{q}j)$ and $\Omega(\mathbf{q}j)$ (for values of $\mathbf{q}$ lying in the principal symmetry directions of the crystal) also allows us to plot the dispersion curves of the crystal, in the QH and RE cases respectively.

### 2.3. Numerical Procedure

The numerical values of the $\omega(\mathbf{q}j)$ and $\mathbf{e}(\mathbf{q}j)$ are obtained from the dynamical matrices $D_{\alpha\beta}(\mathbf{q})$:

$$\omega^2(\mathbf{q}j) = \sum_{\alpha\beta} e_\alpha(\mathbf{q}j) D_{\alpha\beta}(\mathbf{q}) e_\beta(\mathbf{q}j) \tag{19}$$

The method we have used to construct the dynamical matrices is described in detail in Shukla (1966) and Shukla (1980) so we will not reproduce it here.

The quantities $\Delta_3(\mathbf{q}j)$ and $\Delta_4(\mathbf{q}j)$ in equation (13) are evaluated from the following expressions (Shukla and Hübschle 1989a):

$$\Delta_3(\mathbf{q}j) = -\frac{k_B T}{8N^2M^3} \sum_{\alpha\beta} e_\alpha(\mathbf{q}j) e_\beta(\mathbf{q}j) \sum_{\ell} {\sum_{\ell_1,\ell_2}}' g(\mathbf{q};\ell,\ell_1,\ell_2) \sum_{\tau\lambda} \sum_{\sigma\delta} \phi_{\tau\delta\alpha}(\ell_1)\phi_{\lambda\sigma\beta}(\ell_2) \times F_{\tau\lambda}(\ell,\ell_1,\ell_2) F_{\delta\sigma}(\ell,\ell_1,\ell_2) \tag{20}$$

$$\Delta_4(\mathbf{q}j) = \frac{k_B T}{NM^2} \sum_{\alpha\beta} e_\alpha(\mathbf{q}j) e_\beta(\mathbf{q}j) \sum_{\ell_1}{}' [1 - cos(\mathbf{q} \cdot \mathbf{r}_{\ell_1})] \sum_{\gamma\delta} \phi_{\alpha\beta\gamma\delta}(\ell_1)[S_{\gamma\delta}(0) - S_{\gamma\delta}(\ell_1)] \quad (21)$$

where the $S$-tensors are defined by

$$S_{\alpha\beta}(\ell) = \sum_{\mathbf{q}j} \frac{e_\alpha(\mathbf{q}j) e_\beta(\mathbf{q}j)}{\omega^2(\mathbf{q}j)} cos(\mathbf{q} \cdot \mathbf{r}_\ell) \quad (22)$$

and the $F_{\alpha\beta}$ and $g$ functions are defined by

$$F_{\alpha\beta}(\ell, \ell_1, \ell_2) = S_{\alpha\beta}(\ell) - S_{\alpha\beta}(\ell - \ell_1) - S_{\alpha\beta}(\ell + \ell_2) + S_{\alpha\beta}(\ell - \ell_1 + \ell_2) \quad (23)$$

$$g(\mathbf{q}; \ell, \ell_1, \ell_2) = cos(\mathbf{q}\cdot\mathbf{r}_\ell) - cos[\mathbf{q}\cdot(\mathbf{r}_\ell - \mathbf{r}_{\ell_1})] - cos[\mathbf{q}\cdot(\mathbf{r}_\ell + \mathbf{r}_{\ell_2})] + cos[\mathbf{q}\cdot(\mathbf{r}_\ell - \mathbf{r}_{\ell_1} + \mathbf{r}_{\ell_2})] \quad (24)$$

In the argument of $S_{\alpha\beta}(\ell)$, $\ell = 0$ denotes $r_\ell = 0$ (the position of the central lattice site). Since all the information about the $\mathbf{e}(\mathbf{q}j)$ and $\omega(\mathbf{q}j)$ is contained within the $D_{\alpha\beta}(\mathbf{q})$ matrices the $S$-tensors may also be represented in terms of the $D_{\alpha\beta}(\mathbf{q})$ matrices (Shukla and Wilk 1974).

The real-lattice sums over $\ell_1$ in Eq.( 21), and over $\ell_1$ and $\ell_2$ in Eq.( 20), include all neighbouring atoms which lie within the interaction range of the

pair potential. The primes over the summations denote the omission of the central lattice site from these sums.

In theory, the sum over $\ell$ in Eq.( 20) includes all the atoms in the crystal. However, in practice, contributions to $\Delta_3(\mathbf{q}j)$ decrease in magnitude with increasing $r_s$ and the sum over $\ell$ can eventually be truncated after a finite number of neighbour shells. In our calculation of $\Delta_3(\mathbf{q}j)$ for fcc and bcc materials, the values of $\ell$ we have used correspond to 7 and 12 neighbour shells respectively. This was found to produce adequate convergence for $\Delta_3(\mathbf{q}j)$ and for $< u^2 >_C$ which is obtained from the $\Delta_3(\mathbf{q}j)$ as follows:

$$< u^2 >_C = -\frac{k_B T}{NM} \sum_{\mathbf{q}j} \frac{\Delta_3(\mathbf{q}j)}{\omega^2(\mathbf{q}j)} \tag{25}$$

Similarly the quartic anharmonic contribution to MSD is numerically obtained from the $\Delta_4(\mathbf{q}j)$:

$$< u^2 >_Q = -\frac{k_B T}{NM} \sum_{\mathbf{q}j} \frac{\Delta_4(\mathbf{q}j)}{\omega^2(\mathbf{q}j)} \tag{26}$$

The quantities $< u^2 >_{QH}$, $< u^2 >_C$ and $< u^2 >_Q$ can also be evaluated in terms of the $S$-matrices (Shukla and Plint 1989). In this form the expression for $< u^2 >_{QH}$ is (Shukla and Mountain 1982):

$$< u^2 >_{QH} = \frac{k_B T}{NM}[S_{xx}(0) + S_{yy}(0) + S_{zz}(0)] \qquad (27)$$

An alternate method of evaluating $< u^2 >_C$ and $< u^2 >_Q$ (Goldman 1968) involves replacing $\Delta_3(\mathbf{q}j)$ and $\Delta_4(\mathbf{q}j)$ with a $\mathbf{q}j$-independent average frequency shift. We will examine the merits of this frequency shift method in Chapter 3. $< u^2 >_{RE}$ is evaluated by use of Eq.( 14).

In theory the reciprocal lattice sums over $\mathbf{q}$ in Eqs.( 14)-( 17), ( 22), and ( 25)-( 26) range over the entire FBZ of the crystal. However, because the FBZ of a cubic crystal possesses cubic symmetry it is only necessary to consider the wavevectors lying within the irreducible 1/48th section of the FBZ in evaluating these sums. The values of $\mathbf{q}$ used in our calculations make up a simple cubic mesh of wavevectors in the 1/48th FBZ. For the fcc lattice, the co-ordinates of these reciprocal space wavevectors $\mathbf{q} = \frac{\pi}{La_0}\mathbf{p}$ are determined from the relations:

$$L \geq p_x \geq p_y \geq p_z \geq 0; p_x + p_y + p_z < 1.5L \qquad (28)$$

and for the bcc lattice,

$$p_x + p_y \leq L; p_y + p_z \leq L; p_z + p_x \leq L; L \geq p_x \geq p_y \geq p_z \geq 0 \qquad (29)$$

where $\mathbf{p} = (p_x, p_y, p_z)$. Here $p_x, p_y, p_z$ and $L$ are all non-negative integers, $a_0$ is the lattice constant and $L$ is defined to be the step length in the reciprocal lattice. Each wave-vector in the 1/48th section of the FBZ is assigned a weighting factor in order to account for the number of equivalent points in the full FBZ. The central wavevector $\mathbf{q} = 0$ is omitted [because here $\omega(\mathbf{q}j) = 0$] so in practice the normalization factor $N$ is replaced with ($N$-1).

In a real crystal, $L$ is very large so if the calculation of MSD is to be realistic it is desirable to extract the value of the MSD in the limit $L \to \infty$. It has been observed (Heiser, Shukla and Cowley 1986) that the numerical values of MSD vary linearly with $1/L$ so by calculating the MSD for several finite values of $L$ we can obtain the MSD in this limit. In our calculation of MSD for fcc materials, the extrapolation has been performed using step lengths of 6, 8 and 10. For bcc materials, step lengths of 20, 25 and 30 have been used.

# 3. Results for Mean Square Displacement

In this chapter we report the results of calculations of MSD which we have performed for different types of elemental solids. We begin by reporting the results of our calculation of MSD for a fcc Lennard-Jones (L-J) solid (Xe) in which we have used potential parameters fitted to NN and NNN pair interactions. We have summarized the method by which these parameters are determined in order to show why their values depend upon the interaction range of the pair potential. The MSD of Xe has been calculated in the NN and NNN approximations and the NN and NNN results have been compared with each other in order to determine whether the second neighbour interactions are important in the anharmonic calculation of MSD. We also compare our $\lambda^2$ PT results for the MSD of Xe, which have been calculated exactly, with results obtained by Goldman (1968) using a frequency-shift approximation method. We conclude that this approximation method is inadequate in the calculation of MSD to $O(\lambda^2)$.

Next we report our results of MSD for seven fcc metals. These have been carried out in the NN approximation using both the 3 parameter Morse potential and a 4 parameter modified Morse potential. Except in the case of Al

we have only reported the results which were obtained using the 4 parameter modified Morse potential. Finally we describe our calculation of the MSD of five alkali metals and five bcc transition metals. For each of the bcc metals the potential function we have used is either the 3 parameter Rydberg potential or the 4 parameter modified Morse potential. For all the bcc metals our calculations have been carried out in the NNN approximation. In all our calculations of MSD our results have been compared with experimental data wherever it is available.

In this chapter and in Chapter 4 all references to the anharmonic contribution to the MSD and phonon frequencies denote the explicit anharmonic contribution obtained from the Green's function method (and, in the case of MSD, the $\lambda^2$ PT method as well) rather than the implicit anharmonic contribution which is already included in the QH result.

## 3.1 MSD of a Lennard-Jones Solid

### 3.1.1. Potentials and Lattice Constants

In our calculations of the MSD of a L-J solid we have used the familiar 12-6 form of the L-J potential:

$$\phi_{L-J}(r) = \varepsilon \left[ \left( \frac{r_0}{r} \right)^{12} - 2 \left( \frac{r_0}{r} \right)^{6} \right] \tag{30}$$

Here $\varepsilon$ is the well depth and $r_0$ is the position of the minimum of the potential. These potential parameters are obtained from experimental values of the sublimation energy $L_0$ and the zero-temperature lattice constant $r_z$, and satisfy the relations (Shukla and Shanes 1985)

$$U(r_z) + E_h = -L_0 \tag{31}$$

$$\left( \frac{\partial U(r)}{\partial r} \right)_{r=r_z} = 0 \tag{32}$$

where $U(r)$ is the static energy of the L-J potential:

$$U(r) = \frac{1}{2} {\sum_{\ell}}' \phi_{L-J}(|\mathbf{r}_\ell|) \tag{33}$$

and $E_h$ is the zero-point energy.

$$E_h = \frac{1}{2} \hbar \sum_{\mathbf{q}j} \omega(\mathbf{q}j) \tag{34}$$

In Eq.( 33) $\mathbf{r}_\ell$ is the position vector of the $\ell^{th}$ lattice point. The sum over $\ell$ includes all the lattice points which lie within the interaction range of the pair potential. The prime over the summation sign indicates the omission of the central lattice site from the sum. In the NN approximation, the sum

over $\ell$ in Eq.( 33) therefore includes only the 12 nearest neighbours of the fcc crystal, while in the NNN approximation the 6 next-nearest neighbours are also included. Since $U(r)$ therefore depends upon the interaction range of the pair potential it follows that the potential parameters $\varepsilon$ and $r_0$, which are obtained from $U(r)$ and its derivative, are also dependent upon the range of the potential.

The potential parameters we have used in our calculation of MSD are taken from Shukla and Shanes (1985) (for the NN case) and Brown (1965) (for the NNN case). These potential parameters are listed in Table I. The procedure outlined above was used to calculate the parameters of the L-J potential in both these references. The lattice constants for Xe used in our calculations are taken from experimental data in Klein and Venables (1977).

### 3.1.2 Results and Discussion

In Fig. (3.1.1) we present our results for the MSD of Xe. The NN and NNN results, calculated in the QH approximation, are in very good agreement. Near $T_m$ the NNN result is only 2.3% larger than the NN result which indicates that the second neighbour interaction does not have much effect on the QH value of MSD. The agreement between the NN and NNN

Table I. Lennard-Jones Potential Parameters for Xenon

| | $\epsilon$ $(10^{-14} erg)$ | $r_0$ $(\AA)$ |
|---|---|---|
| NN[a] | 4.577 | 4.318 |
| NNN[b] | 4.086 | 4.356 |

[a] Shukla and Shanes (1985)

[b] Brown (1965)

Figure 3.1.1.

Results for the Mean Square

Displacement of Xenon

The solid lines are the results calculated from the NN model. Dashed lines are results from the NNN model. QH, PT and RE refer to quasiharmonic, $\lambda^2$ and renormalized vales of MSD respectively. D denotes Debye temperature and M the melting temperature.

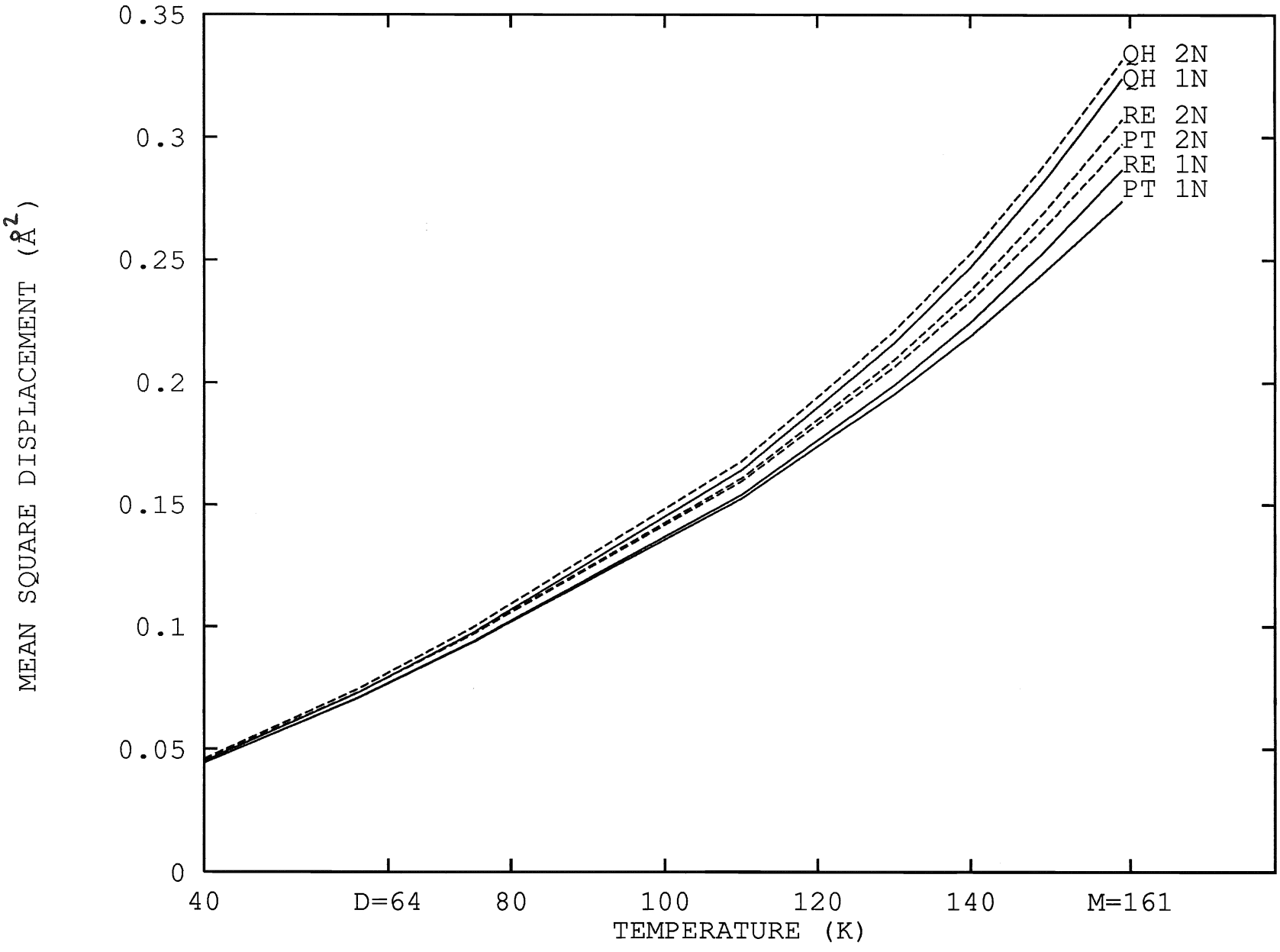
0.35
0.3
0.25
0.2
0.15
0.1
0.05
0
MEAN SQUARE DISPLACEMENT (Å²)
40
D=64
80
100
120
140
M=161
TEMPERATURE (K)
QH 2N
QH 1N
RE 2N
PT 2N
RE 1N
PT 1N

results is however not as good for the $\lambda^2$ PT results for MSD for which the NNN results are 8.5% larger that the NN results near $T_m$. This is due to the fact that the $\lambda^2$ anharmonic contribution to MSD, calculated from the NNN model, only has about two-thirds the magnitude of the $\lambda^2$ anharmonic contribution obtained from the NN model. This happens because the $\lambda^2$ anharmonic contribution to MSD is the sum of two terms ($< u^2 >_C$ and $< u^2 >_Q$) which are of roughly the same magnitude but have opposite sign and which therefore largely cancel each other. Relatively small changes in the values of $< u^2 >_C$ and $< u^2 >_Q$ due to the second neighbour interactions therefore can cause proportionately larger changes in their total. In order to illustrate this, in Tables II(a) and II(b) we have tabulated the values of the QH, cubic and quartic contributions to MSD in the NN and NNN approximations respectively. The $\lambda^2$ anharmonic contribution to MSD (this is the sum of the cubic and quartic contributions), the total $\lambda^2$ PT result and the RE result have also been included in Tables II(a) and II(b) for the sake of completeness.

For the renormalized values of MSD the agreement between NN and NNN results is only slightly better than in the PT case with the NNN result being about 7% larger than the NN result. For the L-J solid the second neighbour

Table II(a). Results for MSD of Xe in the NN Approximation

| T (K) | QH | C | Q | C+Q | $\lambda^2$ PT | RE |
|---|---|---|---|---|---|---|
| 40 | .0451 | .0047 | -0.0055 | -0.0008 | 0.0443 | 0.0444 |
| 60 | .0729 | .0124 | -0.0145 | -0.0021 | 0.0707 | 0.0709 |
| 75 | .0974 | .0223 | -0.0262 | -0.0039 | 0.0935 | 0.0938 |
| 110 | .164 | .0647 | -0.0764 | -0.0117 | 0.152 | 0.154 |
| 120 | .190 | .0877 | -0.104 | -0.0159 | 0.174 | 0.176 |
| 130 | .216 | .115 | -0.136 | -0.0210 | 0.195 | 0.199 |
| 140 | .247 | .152 | -0.180 | -0.0280 | 0.219 | 0.225 |
| 150 | .283 | .203 | -0.240 | -0.0374 | 0.246 | 0.254 |
| 160 | .324 | .270 | -0.320 | -0.0499 | 0.274 | 0.287 |

Table II(b). Results for MSD of Xe in the NNN Approximation

| T (K) | QH | C | Q | C+Q | $\lambda^2$ PT | RE |
|---|---|---|---|---|---|---|
| 40 | .0461 | .0051 | -0.0057 | -0.0006 | 0.0455 | 0.0455 |
| 60 | .0745 | .0133 | -0.0149 | -0.0015 | 0.0729 | 0.0730 |
| 75 | .0995 | .0240 | -0.0268 | -0.0028 | 0.0967 | 0.0970 |
| 110 | .168 | .0696 | -0.0778 | -0.0082 | 0.159 | 0.161 |
| 120 | .194 | .0943 | -0.105 | -0.0112 | 0.183 | 0.185 |
| 130 | .221 | .123 | -0.138 | -0.0147 | 0.207 | 0.209 |
| 140 | .253 | .163 | -0.183 | -0.0194 | 0.233 | 0.238 |
| 150 | .290 | .217 | -0.243 | -0.0257 | 0.264 | 0.271 |
| 160 | .331 | .289 | -0.323 | -0.0340 | 0.297 | 0.307 |

All values of MSD are in units of $\mathring{A}^2$. C and Q denote cubic and quartic anharmonic contributions to MSD.

interactions are therefore important in the anharmonic calculation of MSD but are not so important in the quasiharmonic case.

For the L-J potential the results for MSD can alternately be converted to a dimensionless form in which $T$ and MSD are expressed in units of $\varepsilon/k_B$ and $\sigma^2/1000$ respectively. Here $\sigma$ is the zero position of the L-J potential. (For the 12-6 form of the L-J potential, $\sigma = 2^{-1/6}r_0$.) The advantage of this representation is that for a given value of $r/r_0$ the fully dimensioned MSD can be obtained from the dimensionless value of MSD for any choice of $\varepsilon$ and $r_0$. However, since values of $\varepsilon$ and $r_0$ (calculated using the same values of $L_0$ and $r_z$) are different in the NN and NNN approximations, the dimensionless values of MSD for the NN and NNN cases should not be compared because their units are not the same. In Fig.(3.1.2) we have converted the data of Fig.(3.1.1) to dimensionless form to illustrate this point.

In the past, a number of approximation methods have been used to calculate the anharmonic MSD of rare-gas solids. An example is the frequency-shift method used by Goldman (1968) to obtain the MSD of Xe to $O(\lambda^2)$ for a NN L-J potential. Since our calculation of the MSD of Xe has been done exactly, a comparison of Goldman's results with our $\lambda^2$ PT results will allow us to assess the validity of the frequency-shift method. In these calculations

Figure 3.1.2.

Dimensionless Results for the

Mean Square Displacement of Xenon

The solid lines are the results calculated from the NN model. Dashed lines are results from the NNN model. QH, PT and RE refer to quasiharmonic, $\lambda^2$ and renormalized vales of MSD respectively. Temperatures are expressed in units of $\varepsilon/k_B$ and MSD in units of $\sigma^2/1000$ (see text for definitions).

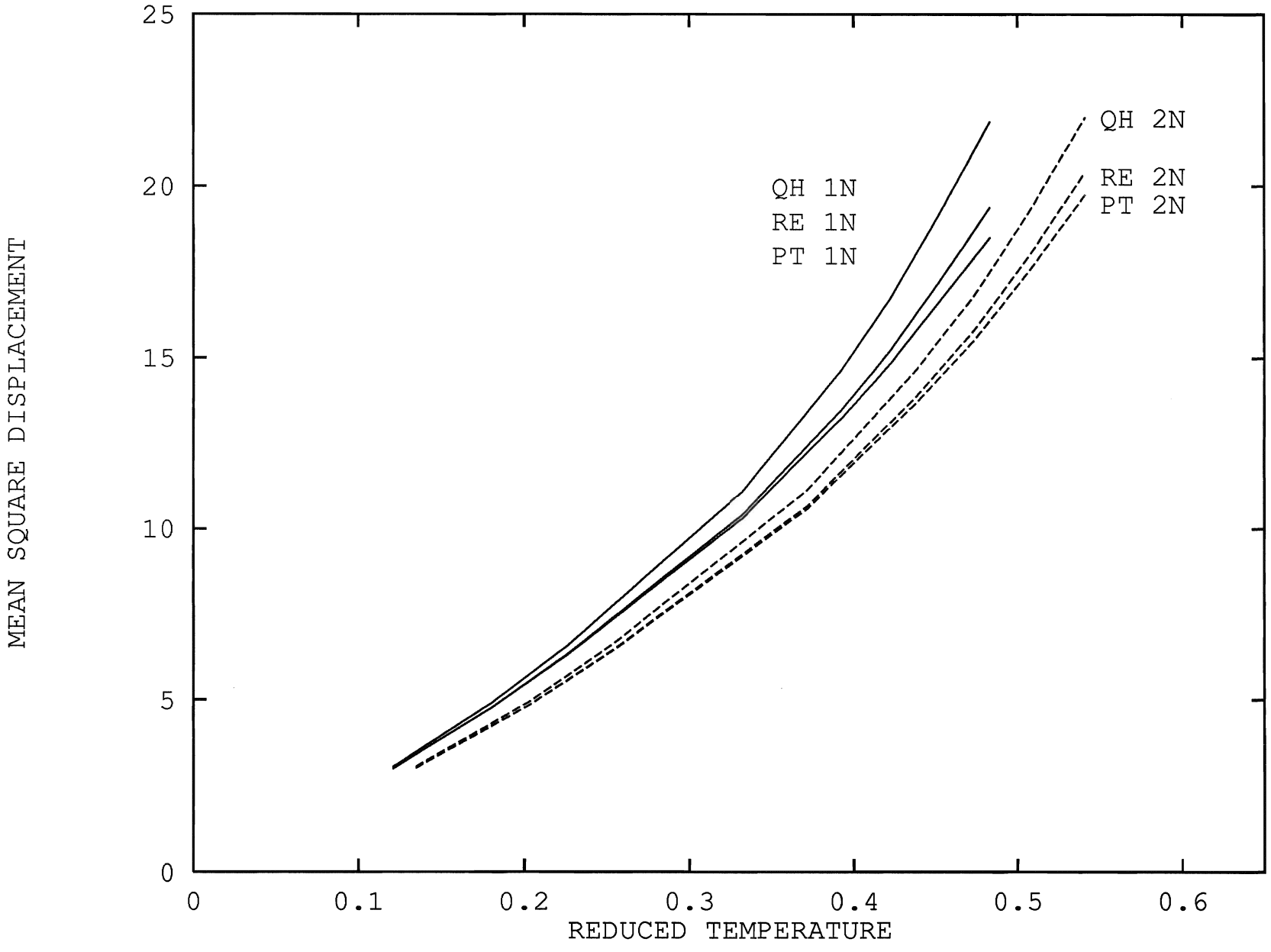
MEAN SQUARE DISPLACEMENT
25
20
15
10
5
0
0
0.1
0.2
0.3
0.4
0.5
0.6
REDUCED TEMPERATURE
QH 1N
RE 1N
PT 1N
QH 2N
RE 2N
PT 2N

we have used the same values of $\varepsilon$, $r_0$ and $L$ used by Goldman in his work ($\varepsilon = 4.576 \times 10^{-14}$ erg, $r_0 = 4.318\mathring{A}$, $L$=20).

In Fig. (3.1.3) we have compared our NN $\lambda^2$ PT results with those of Goldman. Our results disagree with Goldman's at all temperatures above the Debye temperature (where the high-temperature expressions we have used to calculate the QH and anharmonic contributions to the MSD are valid). Near $T_m$, Goldman's results are over 23% below the exact result. The frequency-shift method therefore does not appear to be a very good approximation.

Figure 3.1.3.

Comparison of Theoretical Results

for the Mean Square Displacement

of Xenon

The solid line is the $\lambda^2$ result calculated from the NN model. The dashed line represents the $\lambda^2$ results of Goldman (1968). D denotes the Debye temperature and M the melting temperature.

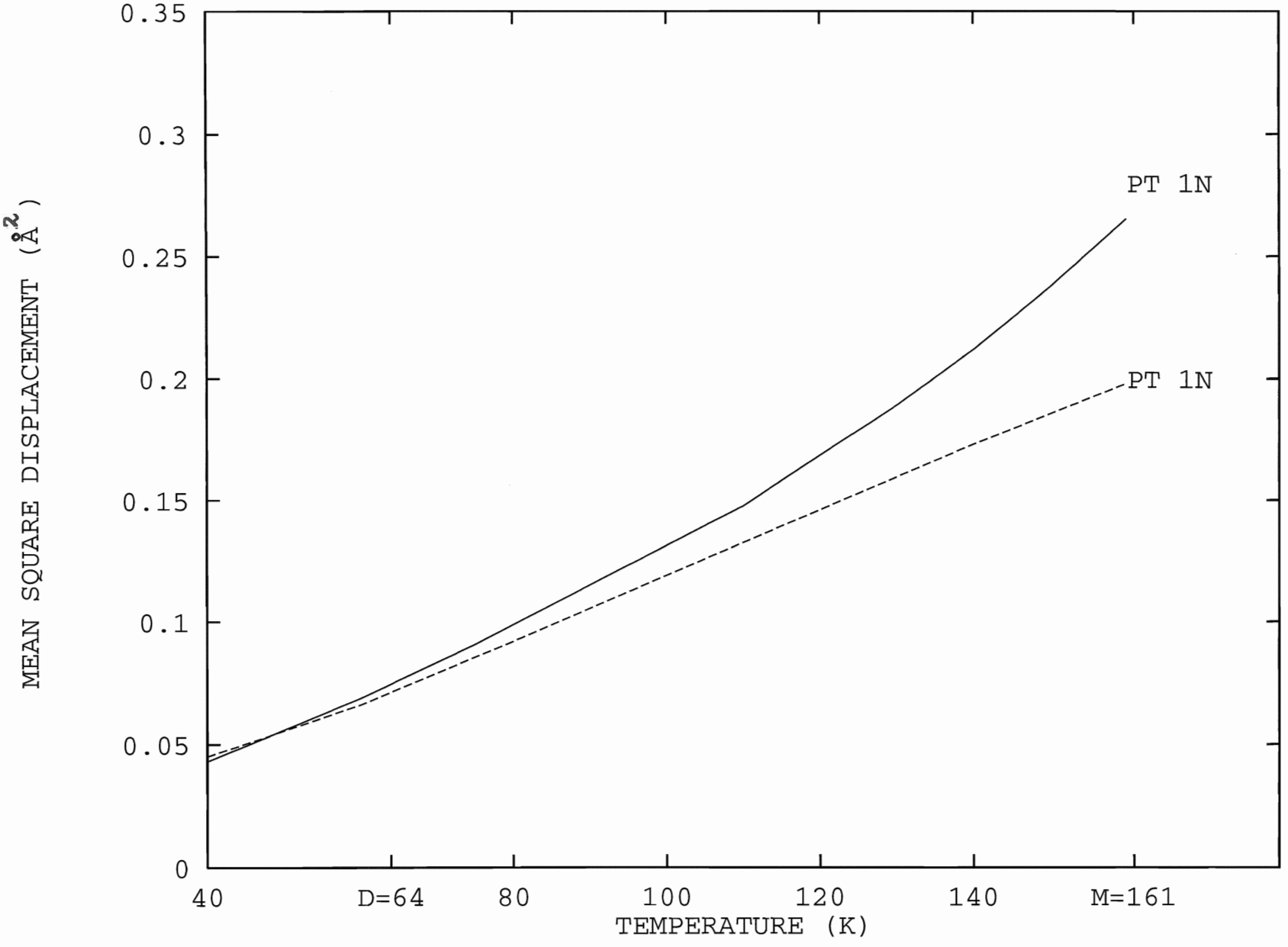
0.35
0.3
0.25
0.2
0.15
0.1
0.05
0
MEAN SQUARE DISPLACEMENT (Å²)
PT 1N
PT 1N
40
D=64
80
100
120
140
M=161
TEMPERATURE (K)

## 3.2 MSD of fcc metals

### 3.2.1 Potentials and Lattice Constants

For all seven fcc metals we have used the 3 parameter Morse potential in our calculation of MSD:

$$\Phi_M(r) = \varepsilon \left( e^{-2\alpha(r-r_0)} - 2e^{-\alpha(r-r_0)} \right) \tag{35}$$

We have also used the 4 parameter (modified) Morse potential:

$$\Phi_{MM}(r) = \frac{\varepsilon}{2b^2 - 1} \left( e^{-2\alpha b(r-r_0)} - 2b^2 e^{-\alpha(r-r_0)/b} \right) \tag{36}$$

The potential parameters $\varepsilon, r_o$, and $\alpha$, which appear in both the 3 and 4 parameter forms of the Morse potential, are determined from experimental values of the sublimation energy, zero-temperature lattice parameter and Debye temperature of the material. The modified Morse potential also contains a fourth parameter, $b^2$, which is obtained from thermal expansion data. (If $b^2$ is set equal to 1 the 4 parameter modified Morse potential of Eq.( 36) reduces to the 3 parameter form of Eq.( 35).) The method by which these potential parameters are determined is outlined in Macdonald, Shukla and Kahaner (1984) (MSK) so we will not repeat it here.

In the L-J case the second-neighbour interactions have already been found to be important in the anharmonic calculation of MSD for a fcc solid. This is however not necessarily the case for other choices of potential function. Shukla (1994) has found that for NN fcc solids, the $\lambda^2$ contribution to MSD obtained from the 3 parameter Morse potential is much smaller than the $\lambda^2$ contribution obtained from the L-J potential. It is likely that this is also true in the NNN approximation in light of the small effect the second neighbour interactions have upon the QH values of MSD. In both the NN and NNN approximations, the anharmonic MSD values obtained from the Morse potential should not differ much from the QH results, and therefore probably do not differ much from each other. In our Morse potential calculations involving the fcc metals we have therefore neglected the second-neighbour interactions in these calculations and used the NN approximation only. Our values of the 3 and 4 parameter Morse potential parameters are taken from Macdonald and Macdonald (1981) who calculated them for the NN case. These parameters are listed in Table III.

The lattice constants used in our calculations are obtained from experimental lattice constants (Pearson 1967) and recommended values of thermal linear expansion (Touloukian 1975).

Table III. Nearest Neighbour Morse Potential

Parameters for the fcc metals

| | $r_0$ ($\AA$) | $\alpha$ ($\AA^{-1}$) | $\epsilon$ ($10^{-12} erg$) | $b^2$ |
|---|---|---|---|---|
| Cu | 2.5471 | 1.1857 | 0.9403 | 2.265 |
| Ag | 2.8675 | 1.1255 | 0.7874 | 2.3 |
| Ca | 3.9264 | 0.8380 | 0.5535 | 1.0 |
| Sr | 4.2804 | 0.7867 | 0.5442 | 1.0 |
| Al | 2.8485 | 1.1611 | 0.6369 | 2.5 |
| Pb | 3.4779 | 0.8350[a] | 0.5500 | 1.5 |
| Ni | 2.4849 | 1.3909 | 0.9843 | 2.4 |

From Macdonald and Macdonald (1981). The parameter $b^2$ is only relevant to the 4 parameter form of the Morse potential (modified Morse).

[a] This entry alone is different in Macdonald and Macdonald. (Shukla, private communication.)

### 3.2.2 Results and Discussion

In Fig. (3.2.1) we present the results of our calculation of the MSD of Al which were carried out using the 3 parameter Morse potential and the 4 parameter modified Morse potential. For clarity only the QH and RE curves have been included in Fig. (3.2.1).

In the QH case, the results for MSD calculated using the 3 parameter Morse potential differ considerably from those calculated using the 4 parameter modified Morse potential. Near $T_m$, the 4 parameter QH results are 6% larger than the 3 parameter QH results. However, in both the $\lambda^2$ PT and RE cases the 3 parameter and 4 parameter results are not very different with the 4 parameter results being about 2% larger. In the case of Al the extra parameter of the 4 parameter modified Morse potential therefore does not provide much additional anharmonicity and only serves to push up the QH curve. This is also true in the cases of Cu, Ni, and Ag. In the case of Pb the values of MSD calculated using the 3 parameter and 4 parameter forms of the Morse potential are not very different regardless of whether the method used is the QH approximation, $\lambda^2$ PT or the Green's function method. For these metals we have therefore only presented the values of MSD which we have

Figure 3.2.1.

Comparison of Theory with Experiment for

the Mean Square Displacement of Aluminum

The solid lines are the values of MSD calculated from the 4 parameter Morse potential. 4QH and 4RE denote the QH and RE results respectively.
The dashed lines are the values of MSD calculated from the 3 parameter Morse potential. 3QH and 3RE again denote the QH and RE results respectively.
The points represent the experimental data of Killean (1974). D denotes the Debye temperature and M the melting temperature.

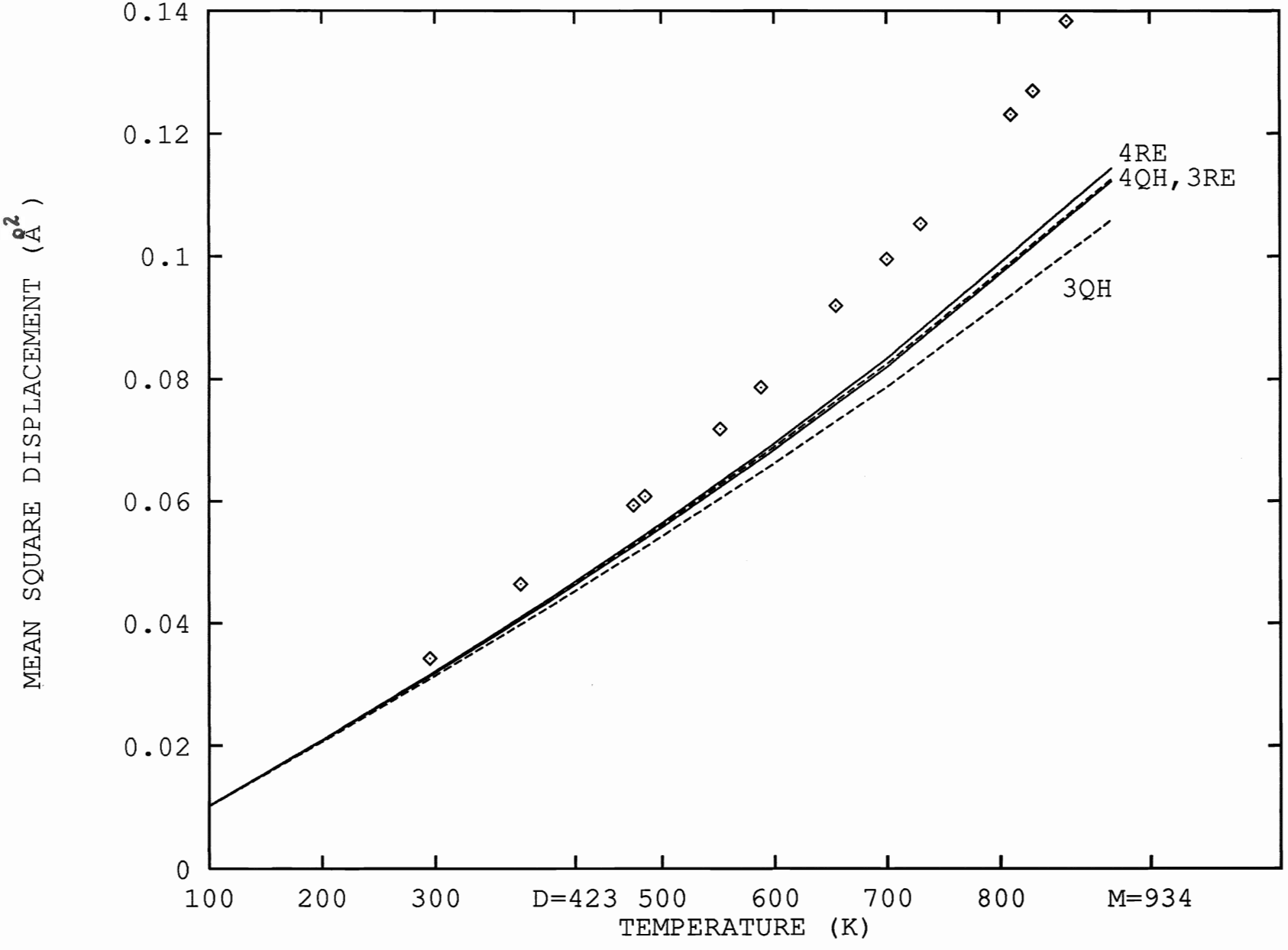
0.14
0.12
0.1
0.08
0.06
0.04
0.02
0
MEAN SQUARE DISPLACEMENT ($Å^2$)
4RE
4QH, 3RE
3QH
100
200
300
D=423
500
600
700
800
M=934
TEMPERATURE (K)

calculated using the 4 parameter modified Morse potential, which overall are in better agreement with experiment than the results obtained from the 3 parameter Morse potential. This has been done to avoid redundancy and to clarify our results and their comparison with experiment.

For Al our results agree well with the experimental data of Killean (1974) at RT but at higher temperatures the experimental data curve upwards from our results. For both the 3 parameter and 4 parameter forms of the Morse potential the $\lambda^2$ PT and RE curves produce successive improvements (in comparison with the QH results) in the agreement between our results and the experimental data, but in the case of the RE anharmonic contribution to MSD this improvement is clearly negligible when compared with the difference between the QH and experimental curves. The situation is similar for the $\lambda^2$ PT results which have been omitted from Fig.(3.2.1).

For Cu (Fig. 3.2.2) our results agree well with the experimental data of Martin and O'Connor (1978) but only at low temperatures. At temperatures above 600 K our QH results fall short of the experimental data. The inclusion of the anharmonicity improves the agreement between theory and experiment to some extent; however, near $T_m$ the RE anharmonic contribution to MSD only accounts for about one-fifth of the discrepancy between our QH results

Figure 3.2.2.

Comparison of Theory with Experiment for

the Mean Square Displacement of Copper

The solid lines are the QH, $\lambda^2$ PT and

RE results calculated from the modified Morse

potential. The points represent the experimental

data of Martin and O'Connor (1978). D denotes the

Debye temperature and M the melting temperature.

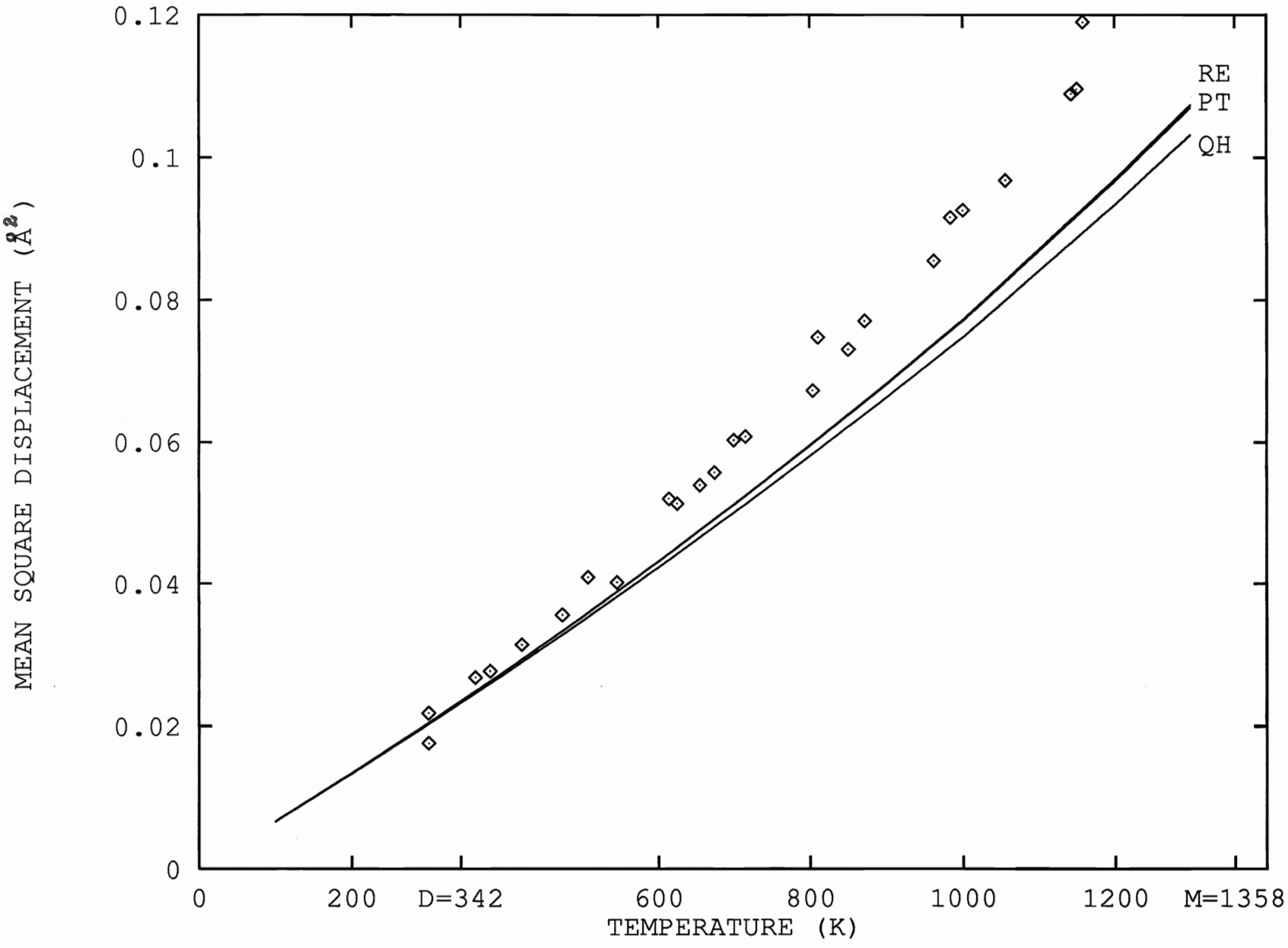
0.12
0.1
0.08
0.06
0.04
0.02
0
MEAN SQUARE DISPLACEMENT (Å²)
RE
PT
QH
0
200
D=342
600
800
1000
1200
M=1358
TEMPERATURE (K)

and the experimental data. The $\lambda^2$ PT curve lies slightly below the RE curve, which is in the best agreement with experiment.

In the case of Pb (Fig. 3.2.3) our MSD curves agree well with the experimental data of Merisalo et al.(1984) and Lisher (1976) at low temperatures, but above 300 K this agreement worsens until, near the melting point, the QH values of MSD are over one-third lower than the experimental value of MSD. The RE curve is in the best agreement with experiment but the RE anharmonic contribution to MSD still accounts for less than one-tenth of the discrepancy between the QH curve and the 550 K experimental point.

For Ag (Fig. 3.2.4) our results agree well with the experimental data of Simerska (1961) up to 900 K, and in this temperature range the anharmonic MSD curves are also in better agreement with the experimental results than the QH curve although the anharmonic contribution to MSD is not very large. Above 900 K all of our results fall short of the experimental data but the anharmonic contribution to MSD still improves the agreement between our results and the experimental data to some extent, with the RE results being in slightly better agreement with experiment than the $\lambda^2$ PT results.

For Ni (Fig. 3.2.5) the experimental data (Singh and Sharma 1971) is only available up to approximately $T_m/2$. At low temperature our results

Figure 3.2.3.

Comparison of Theory with Experiment for the Mean Square Displacement of Lead

The solid lines are the QH, $\lambda^2$ PT and RE results calculated from the modified Morse potential. The points represent the experimental data of Lisher (1976). The crosses are some low-temperature experimental results of Merisalo et. al. (1984) D denotes the Debye temperature and M the melting temperature.

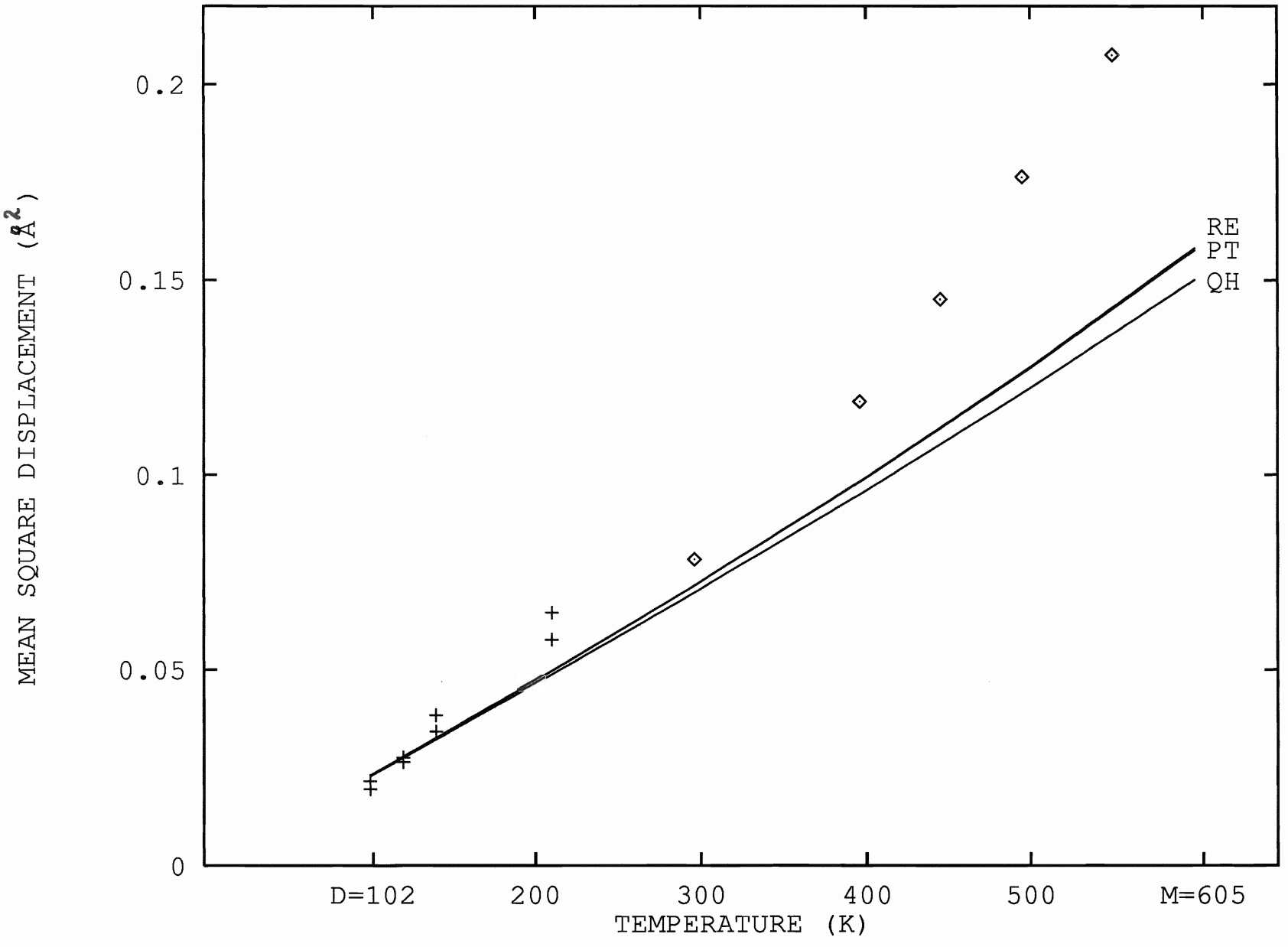
MEAN SQUARE DISPLACEMENT (Å²)
0.2
0.15
0.1
0.05
0
D=102
200
300
400
500
M=605
TEMPERATURE (K)
RE
PT
QH

Figure 3.2.4.

Comparison of Theory with Experiment for the Mean Square Displacement of Silver

The solid lines are the QH, $\lambda^2$ PT and RE results calculated from the modified Morse potential. The points represent the experimental data of Simerska et al. (1961). D denotes the Debye temperature and M the melting temperature.

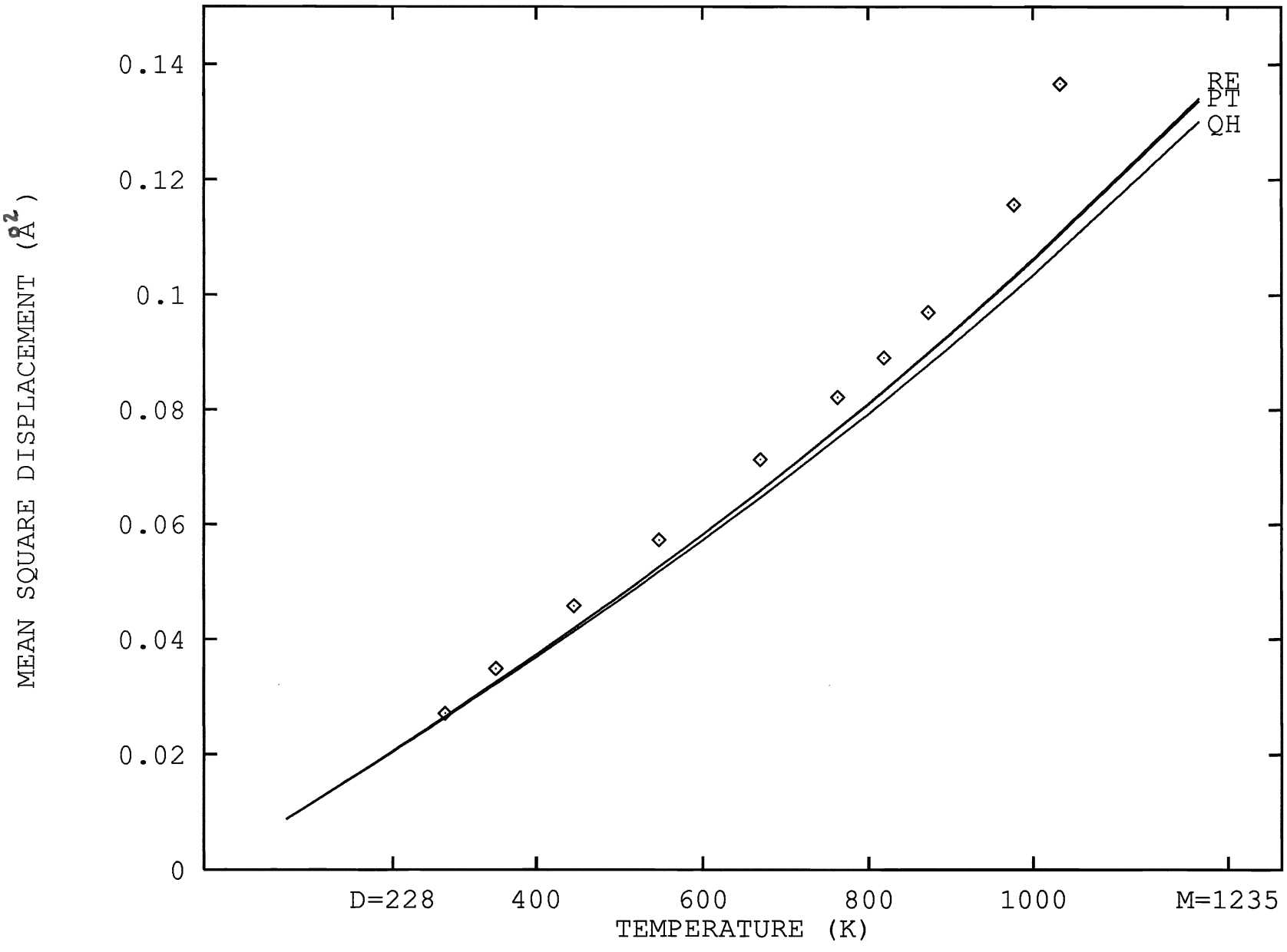
MEAN SQUARE DISPLACEMENT (Å²)
0.14
0.12
0.1
0.08
0.06
0.04
0.02
0
D=228
400
600
800
1000
M=1235
TEMPERATURE (K)
RE
PT
QH

Figure 3.2.5.

Comparison of Theory with Experiment for

the Mean Square Displacement of Nickel

The solid lines are the QH, $\lambda^2$ PT and

RE results calculated from the modified Morse

potential. The points represent the experimental

data of Singh and Sharma (1971). D denotes the

Debye temperature and M the melting temperature.

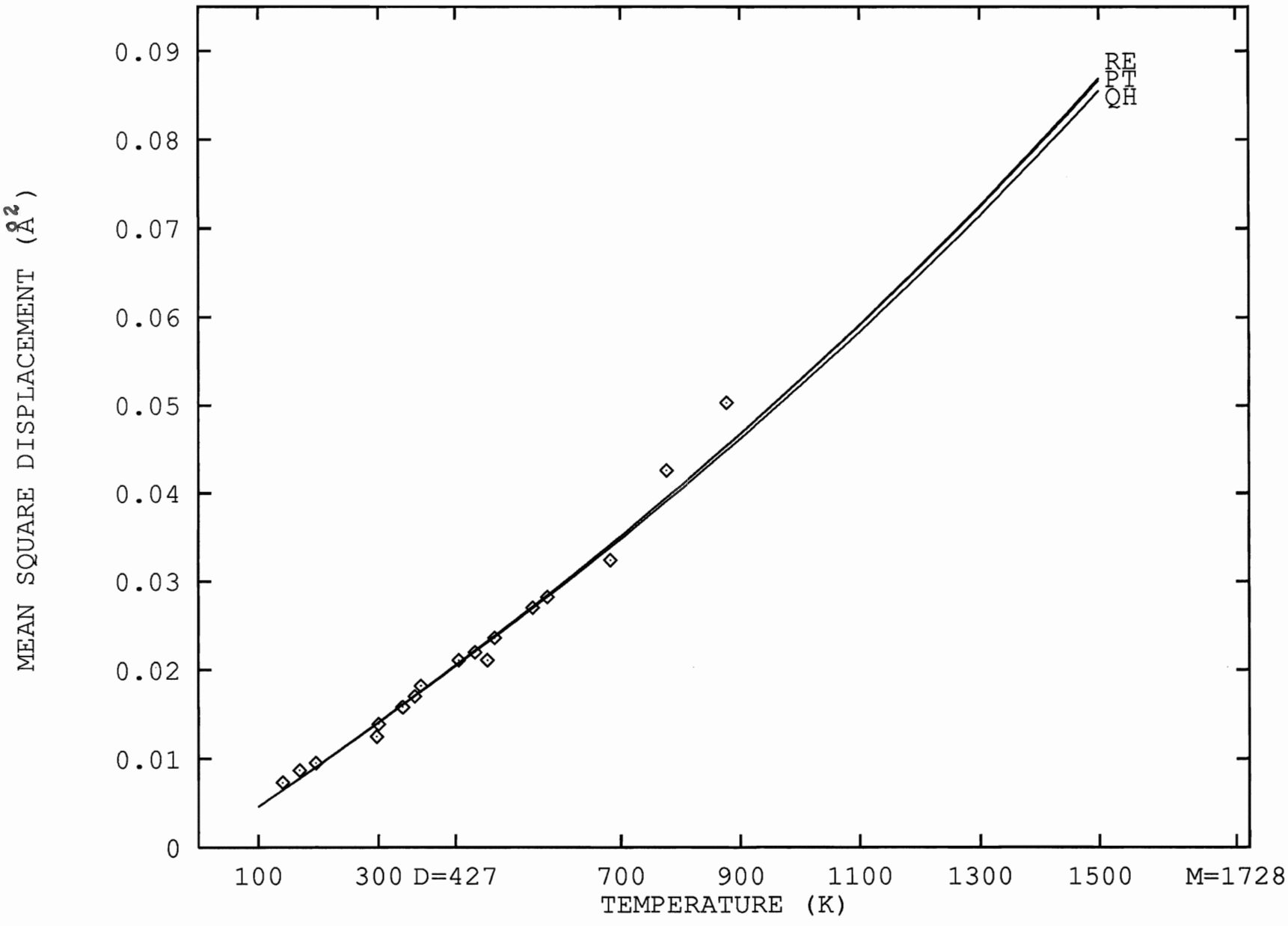
MEAN SQUARE DISPLACEMENT (Å²)
0.09
0.08
0.07
0.06
0.05
0.04
0.03
0.02
0.01
0
100
300
D=427
700
900
1100
1300
1500
M=1728
TEMPERATURE (K)
RE
PT
QH

agree very well with experiment, but even at $T_m/2$ the experimental data is already curving upward from our QH curve as in the cases of Al, Cu, Pb and Ag. The $\lambda^2$ and RE anharmonic contributions to MSD improve the agreement between theory and experiment to some extent but even near $T_m$ the anharmonic corrections are not very large.

In general, for the fcc metals the $\lambda^2$ and RE anharmonic contributions to MSD produce a qualitative improvement in the agreement between theory and experiment, with this agreement being best for the RE results. However, the anharmonic contribution to MSD does not account for much of the observed difference between the experimental data and the QH results. This is particularly true near $T_m$. In this respect alone, the results for MSD which we have obtained using the 3 parameter form of the Morse potential are better than those obtained using the 4 parameter modified form of the potential as can be seen in Fig.(3.2.1). However, since the values of MSD calculated using the 4 parameter modified Morse potential are still in the best overall agreement with the experimental data, we have chosen to concentrate on these rather than on the 3 parameter results.

For all five of the fcc metals for which comparison with experiment is possible, the RE values of MSD are not very different from the $\lambda^2$ PT results

within the temperature range of the experimental data, which indicates that the $\lambda^2$ PT results adequately represent the anharmonic contributions to MSD for these metals and this choice of potential function.

For Ca and Sr no experimental values of MSD could be located in the literature. We have presented the results of our calculations of the MSD of Ca and Sr in Figs. (3.2.6) and (3.2.7) respectively. For Sr the thermal expansion data is only available up to about $T_m/3$. For these two metals the parameter $b^2$ is equal to 1.0 and therefore there is no difference between the 3 parameter Morse and 4 parameter modified Morse potential.

Figure 3.2.6.

Results for the Mean Square

Displacement of Calcium

The solid lines are the QH, $\lambda^2$ PT and

RE results calculated from the modified Morse

potential. D denotes the Debye temperature.

Calcium changes to a bcc structure at 720 K and

melts at 1113 K.

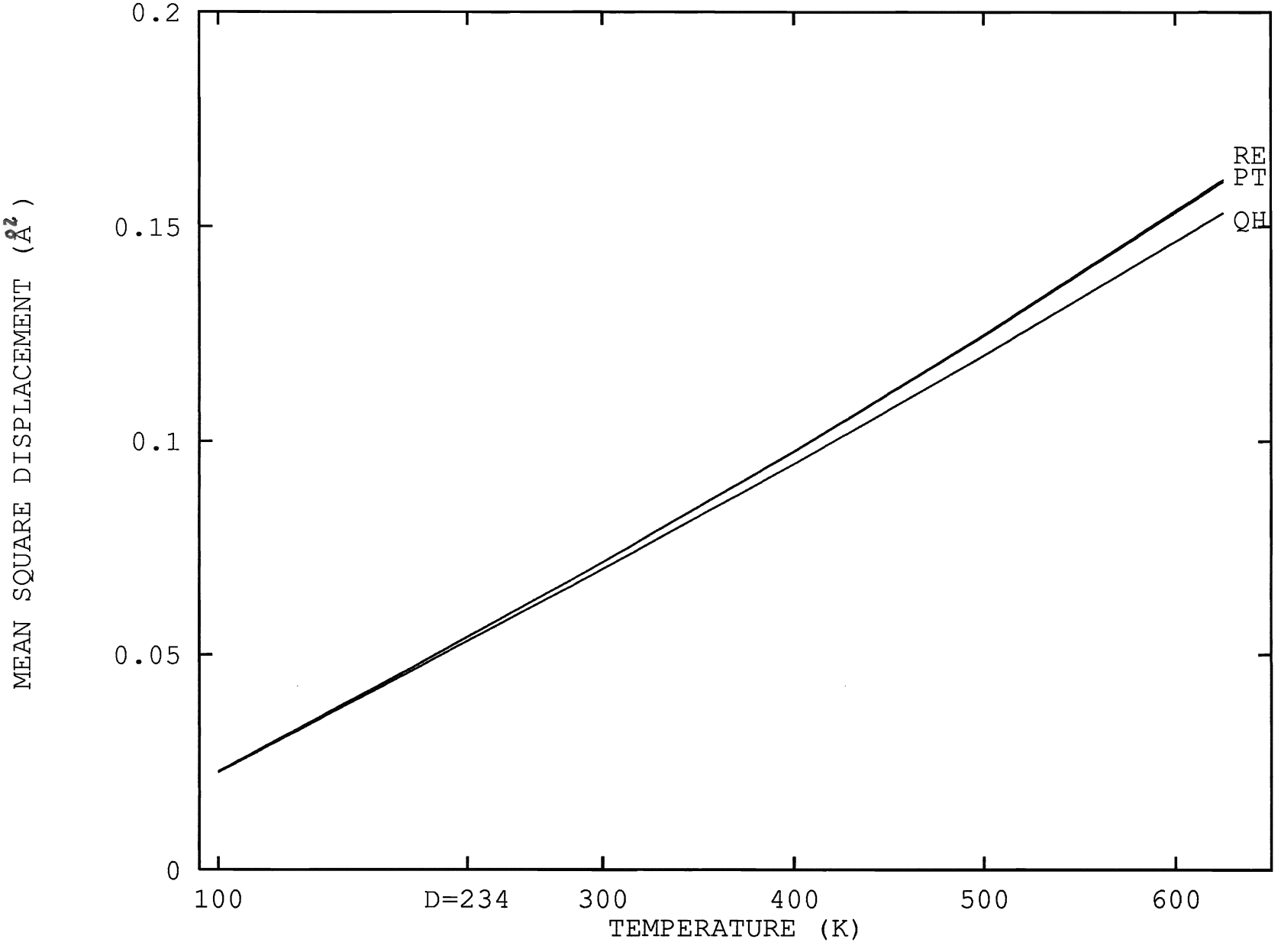
0.2
0.15
0.1
0.05
0
MEAN SQUARE DISPLACEMENT (Å²)
RE
PT
QH
100
D=234
300
400
500
600
TEMPERATURE (K)

Figure 3.2.7.

Results for the Mean Square

Displacement of Strontium

The solid lines are the QH, $\lambda^2$ PT and RE results calculated from the modified Morse potential. D denotes the Debye temperature. Strontium changes to a bcc structure at 830 K and melts at 1042 K.

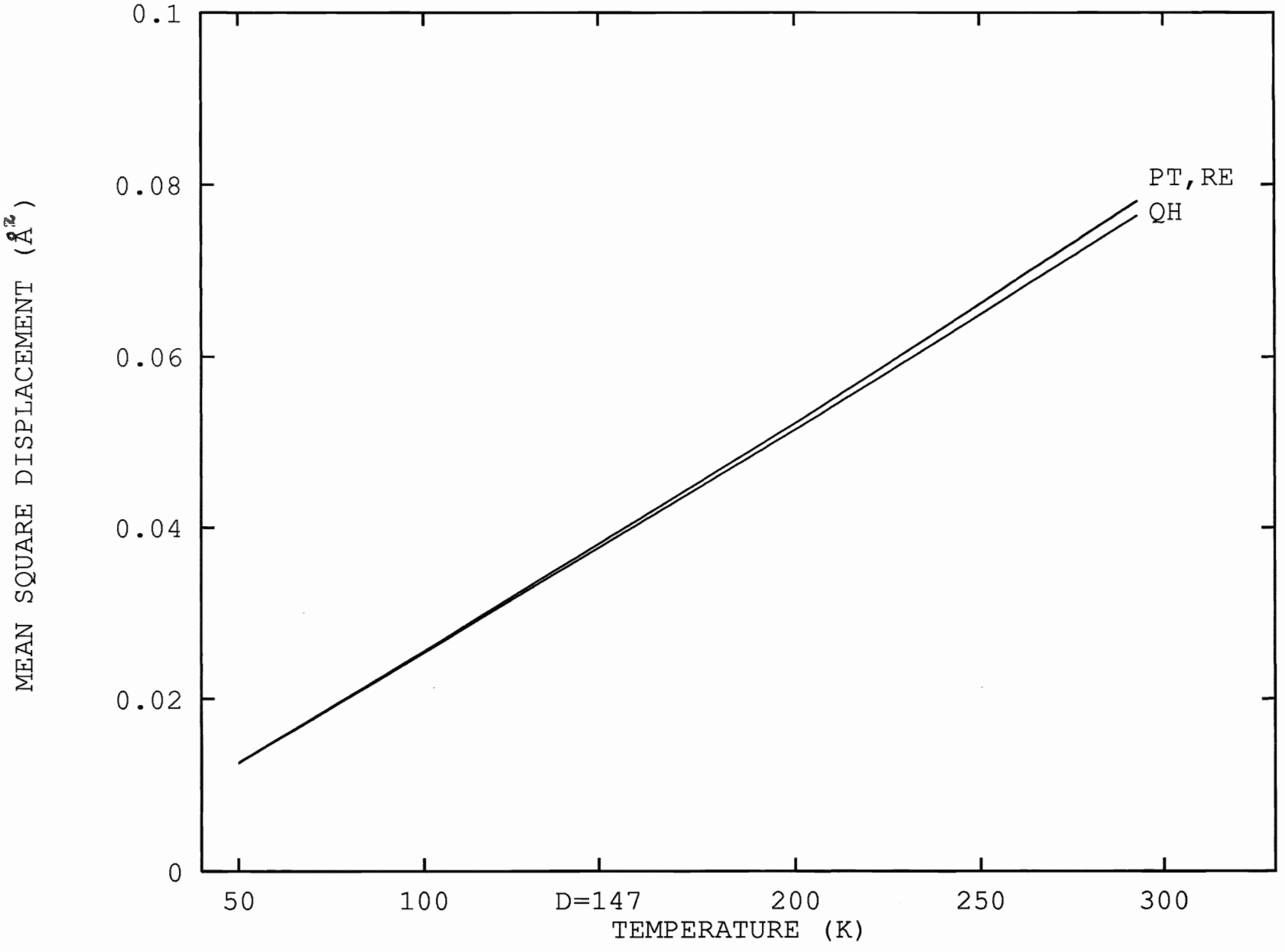
0.1
0.08
0.06
0.04
0.02
0
MEAN SQUARE DISPLACEMENT (Å²)
PT, RE
QH
50
100
D=147
200
250
300
TEMPERATURE (K)

## 3.3 MSD of the bcc alkali metals

### 3.3.1 Potentials and Lattice Constants

The thermodynamic properties of the alkali metals have been calculated, using both the 3 parameter Rydberg potential and the 4 parameter modified Morse potential, by MSK. They found that in the cases of Li, Na, K and Rb, the thermodynamic properties calculated using the modified Morse potential were generally in better agreement with experimental data than those obtained using the Rydberg potential. For Cs alone the Rydberg potential produced better results. In light of the findings of MSK we have used the modified Morse potential of Eq.( 36) in our calculation of MSD for Li, Na, K and Rb.

For Cs we have used the Rydberg potential:

$$\phi_R(r) = -\varepsilon[1 + \alpha(r - r_0)]e^{-\alpha(r-r_0)} \tag{37}$$

The Rydberg potential parameters $\varepsilon$, $\alpha$ and $r_0$ are determined by the same method used to obtained the parameters of the Morse potential. In our calculation of the MSD of the alkali metals we have used the potential parameters of MSK (Table II of their paper). These are listed in Table IV.

Table IV. Next Nearest Neighbour Potential

Parameters for the bcc alkali metals

| | $r_0$ ($\AA$) | $\alpha$ ($\AA^{-1}$) | $\epsilon$ ($10^{-12} erg$) | $b^2$ |
|---|---|---|---|---|
| Li | 3.16089 | 0.63220 | 0.39466 | 2.50 |
| Na | 3.83530 | 0.62804 | 0.26427 | 2.35 |
| K | 4.75468 | 0.53458 | 0.20277 | 1.15 |
| Rb | 5.08217 | 0.48863 | 0.19328 | 1.30 |
| Cs | 5.51053 | 0.64104 | 0.19239 | |

From Macdonald, Shukla and Kahaner (1984). The 4 parameter modified Morse potential is used for Li, Na, K and Rb. For Cs the 3 parameter Rydberg potential is used.

All of the values of lattice constant used in our calculation of MSD for the bcc alkali metals are taken from room-temperature experimental values of the lattice constant (Pearson 1967) and recommended values of thermal linear expansion (Touloukian 1975) except in the case of Rb for which our lattice constants are taken from the experimental work of Copley and Brockhouse (1973), Copley et al. (1974) and Rosengren and Johansson (1975).

### 3.3.2 Results and Discussion

Our results for MSD of the alkali metals are plotted in Figures (3.3.1) through (3.3.5) for Li, Na, K, Rb and Cs respectively. For Li, Na and K experimental values of MSD are available for comparison with our results. In the case of K we have also included results for MSD which were calculated by SH1 using the AVS pseudopotential.

In the case of Li (Fig. 3.3.1), our QH MSD curve is in poor agreement with the experimental data of Bednarz and Field (1982b). Inclusion of the anharmonic contribution to MSD improves this agreement to some extent, with the RE results being in slightly better agreement with experiment than the $\lambda^2$ PT results. However, in the $\lambda^2$ PT case the anharmonic contribution to MSD accounts for only 18% of the difference between the QH value and

Figure 3.3.1.

Comparison of Theory with Experiment for

the Mean Square Displacement of Lithium

The solid lines are the QH, $\lambda^2$ PT and RE results calculated from the modified Morse potential. The point represents the experimental datum of Bednarz and Field (1982b). D denotes the Debye temperature and M the melting temperature.

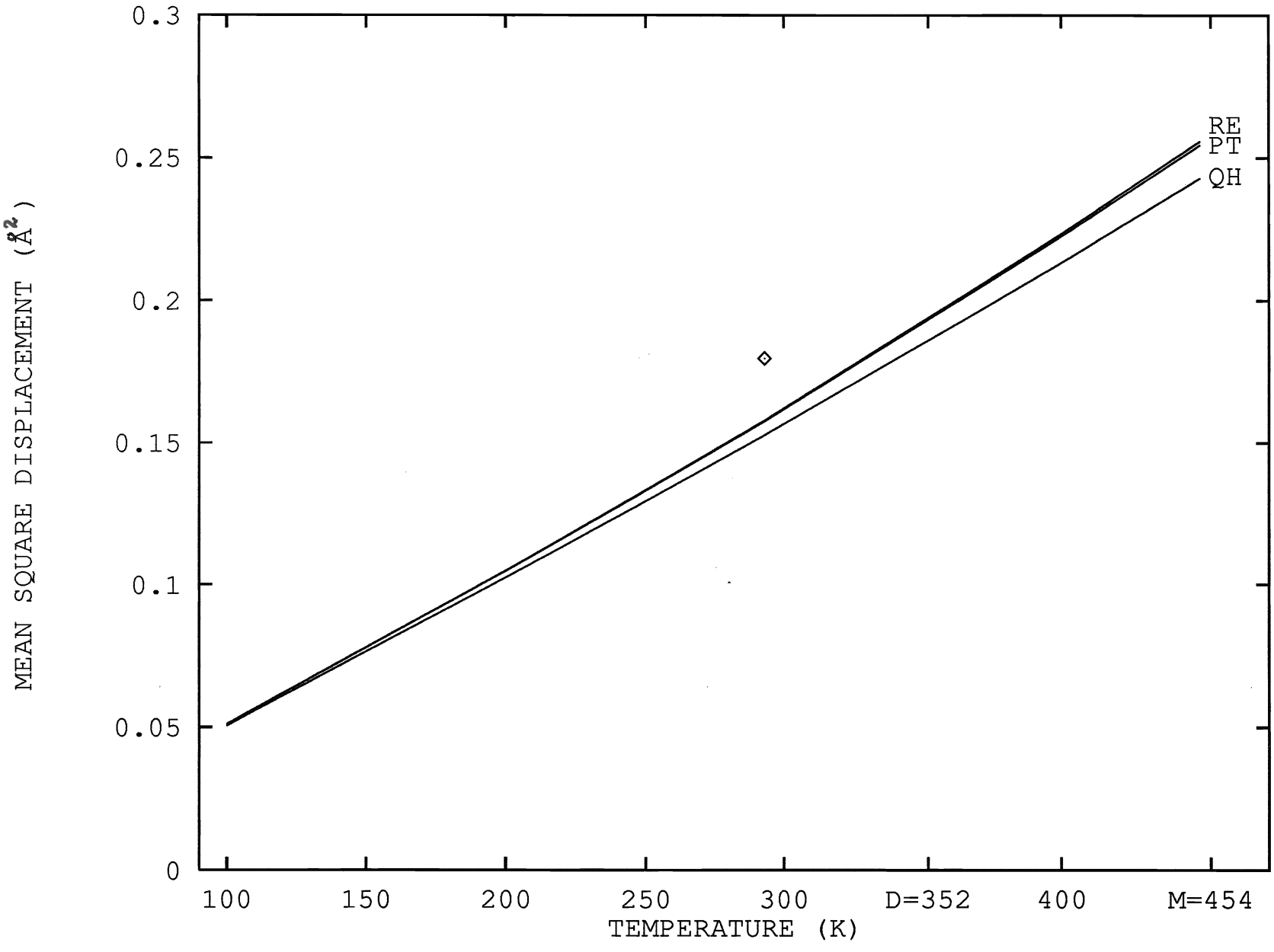
0.3
0.25
0.2
0.15
0.1
0.05
0
MEAN SQUARE DISPLACEMENT (Å²)
RE
PT
QH
100
150
200
250
300
D=352
400
M=454
TEMPERATURE (K)

the room-temperature (RT) experimental point, and in the RE case the anharmonic contribution accounts for only 19% of this difference. Thus there is little quantitative improvement in the agreement between theory and experiment. The RE values of MSD differ only slightly from the $\lambda^2$ PT results near room temperature and only become significantly larger at higher temperatures. For Li the higher-order anharmonic contributions to MSD which are accounted for by the Green's function method therefore do not appear to be very important at RT.

In the case of Na (Figure 3.3.2), the values of MSD obtained from the modified Morse potential are in good agreement with the experimental data of Crow et al. (1989) at temperatures below 200 K. At temperatures above 200 K our values of MSD fall short of the experimental results. As in the case of Li, for Na the anharmonic contribution to MSD produces qualitative improvement in the agreement between theory and experiment (with the RE results being best) but this improvement is negligible.

For K (Fig.3.3.3) we have included the results of SH1 (calculated using the AVS pseudopotential) along with our modified Morse potential results for MSD in order to demonstrate the effect of the choice of potential function upon the agreement between theory and experiment for the bcc metals.

Figure 3.3.2.

Comparison of Theory with Experiment for

the Mean Square Displacement of Sodium

The solid lines are the QH, $\lambda^2$ PT and

RE results calculated from the modified Morse

potential. The point represents the experimental

data of Crow et al. (1989). D denotes the Debye

temperature and M the melting temperature.

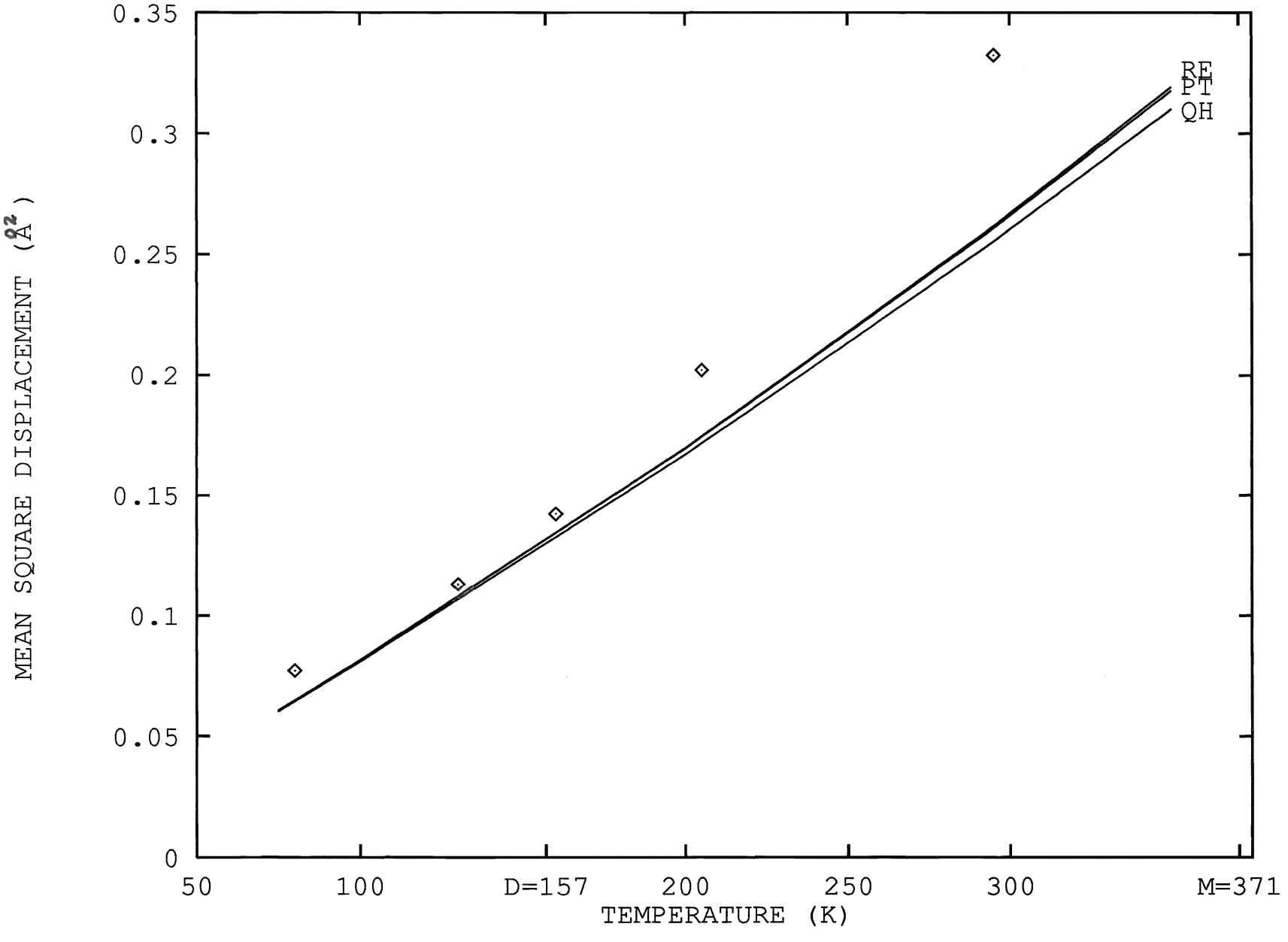
0.35
0.3
0.25
0.2
0.15
0.1
0.05
0
MEAN SQUARE DISPLACEMENT (Å²)
50
100
D=157
200
250
300
M=371
TEMPERATURE (K)
RE
PT
QH

Figure 3.3.3

Comparison of Theory with Experiment for
the Mean Square Displacement of Potassium

The solid lines are the QH, $\lambda^2$ PT and
RE results calculated from the modified Morse
potential. The dashed lines are the QH and
$\lambda^2$ PT results of SH1 calculated from
the AVS potential. The point represents the
experimental datum of Bednarz and Field (1982a).
D denotes the Debye temperature and M the melting
temperature.

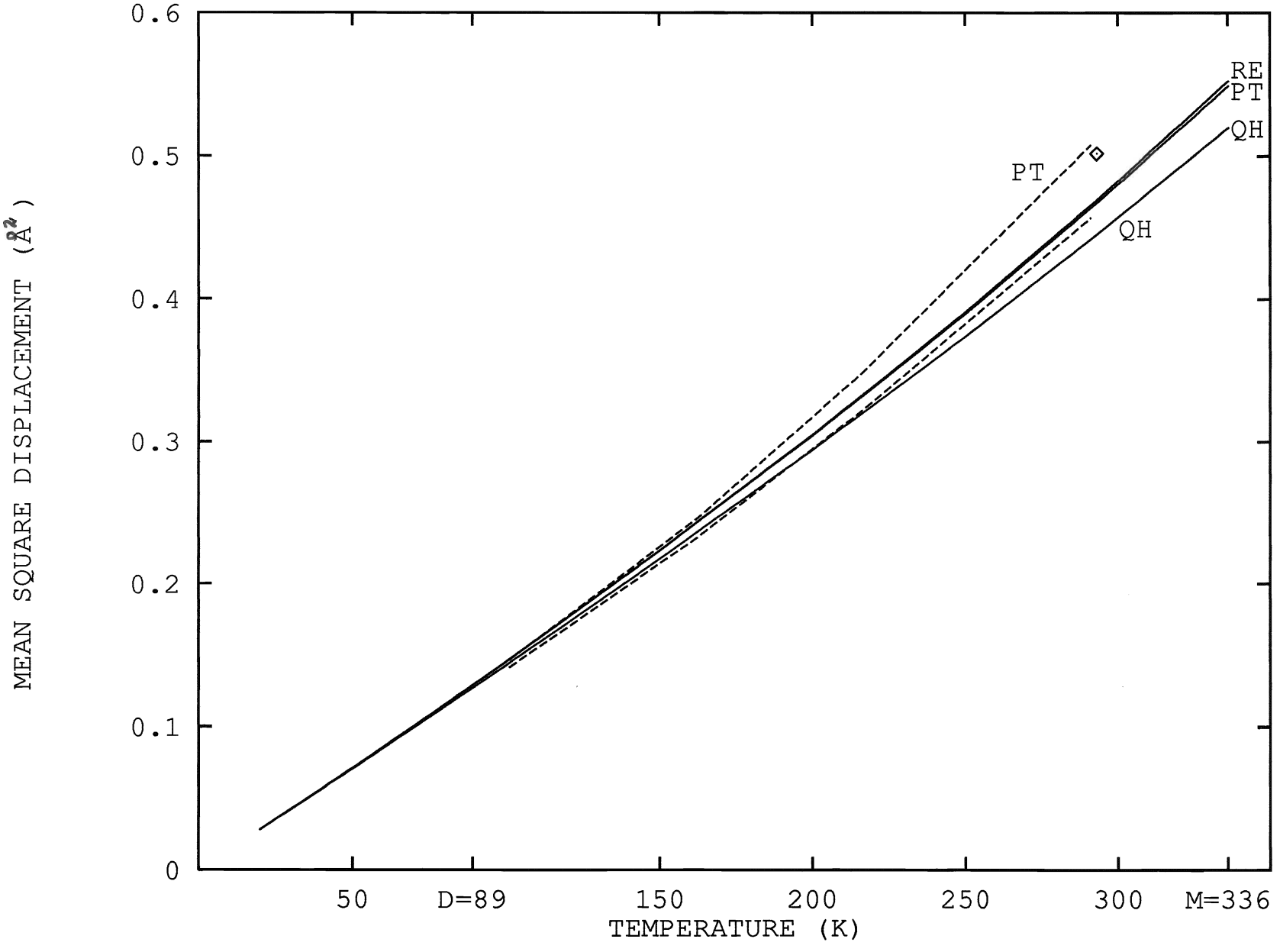
MEAN SQUARE DISPLACEMENT (Å²)
0.6
0.5
0.4
0.3
0.2
0.1
0
50
D=89
150
200
250
300
M=336
TEMPERATURE (K)
RE
PT
QH
PT
QH

The QH values of MSD which we have obtained from the modified Morse potential are in excellent agreement with the QH AVS results of SH1, but in the $\lambda^2$ PT case the anharmonic contribution to MSD produced by the AVS pseudopotential is larger than that produced by the modified Morse potential. Because of this, the AVS $\lambda^2$ PT results are in better agreement with the experimental data (Bednarz and Field 1982a) than our Morse $\lambda^2$ PT results. For the modified Morse potential the RE values of MSD are in the best agreement with experiment, but these still fall short of the AVS $\lambda^2$ PT results.

For Rb (Fig. 3.3.4) and Cs (Fig. 3.3.5) no experimental values of MSD could be located in the literature for comparison with our results.

For the alkali metals, the inclusion of the anharmonic contribution to MSD improves the agreement between the available experimental data and the results we have obtained using the modified Morse potential. The RE results produce the best agreement between theory and experiment. However, in all cases the anharmonic contribution to MSD is not large enough to account for very much of the discrepancy between the QH result and the experimental data.

Figure 3.3.4.

Results for the Mean Square

Displacement of Rubidium

The solid lines are the QH, $\lambda^2$ PT and

RE results calculated from the modified Morse

potential. D denotes the Debye temperature and

M the melting temperature.

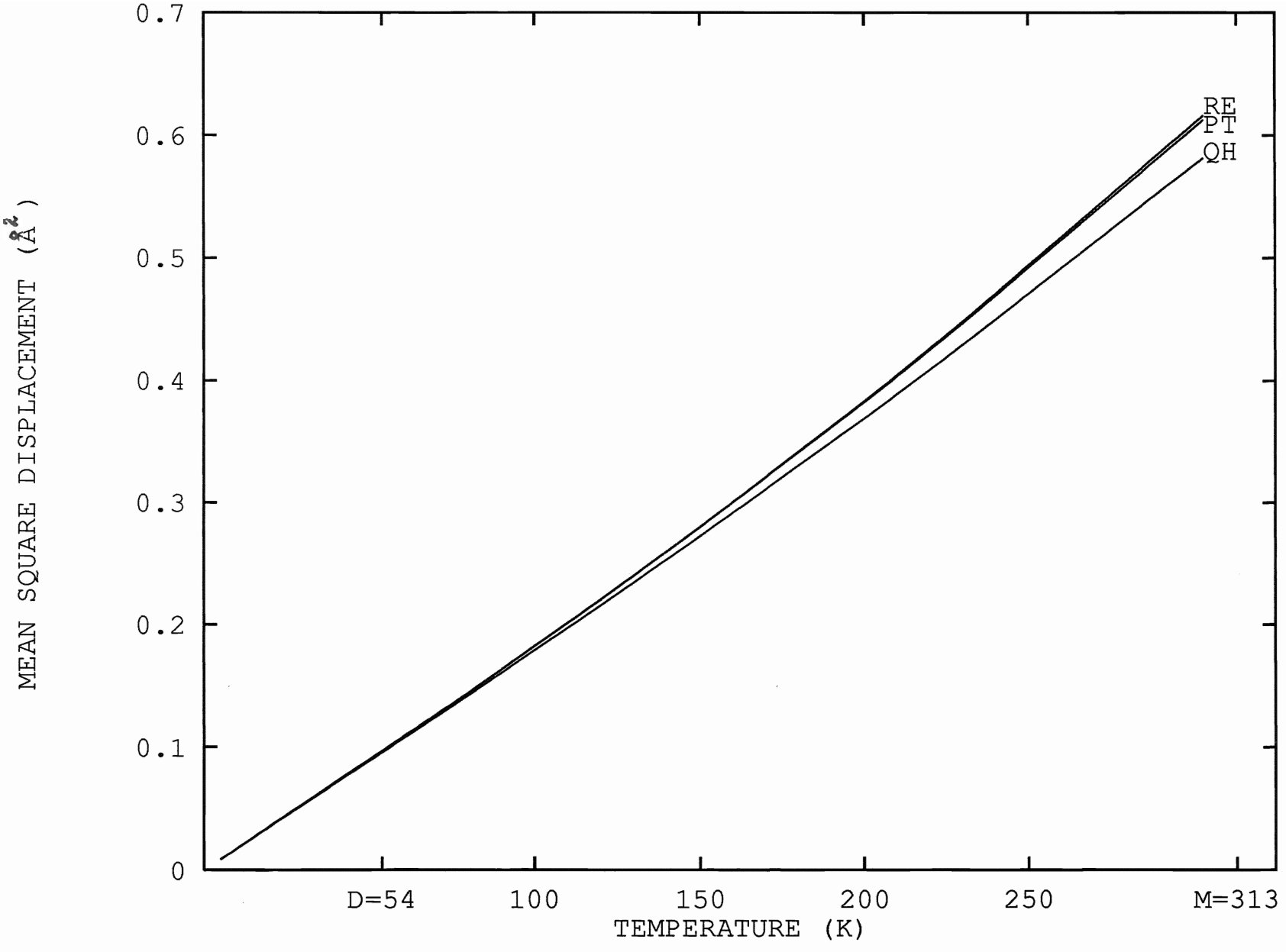
MEAN SQUARE DISPLACEMENT (Å²)
0.7
0.6
0.5
0.4
0.3
0.2
0.1
0
RE
PT
QH
D=54
100
150
200
250
M=313
TEMPERATURE (K)

Figure 3.3.5.

Results for the Mean Square

Displacement of Cesium

The solid lines are the QH, $\lambda^2$ PT

and RE results calculated from the Rydberg

potential. M denotes the melting temperature.

The Debye temperature of Cesium is 40 K.

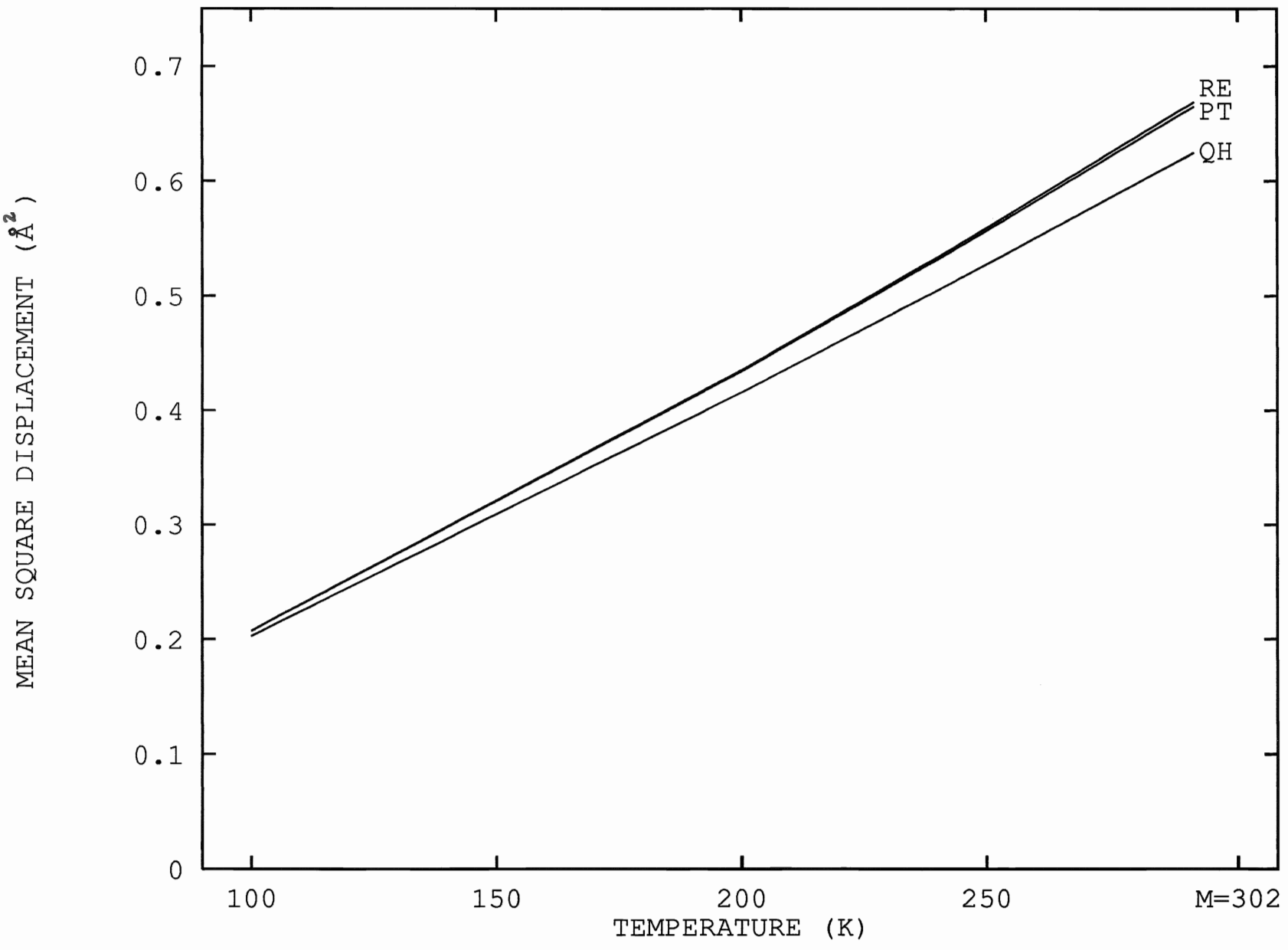
MEAN SQUARE DISPLACEMENT (Å²)
0.7
0.6
0.5
0.4
0.3
0.2
0.1
0
RE
PT
QH
100
150
200
250
M=302
TEMPERATURE (K)

## 3.4 MSD for the bcc transition metals

### 3.4.1. Potentials and Lattice Constants

In our calculations of the MSD of five bcc transition metals (V, Nb, Ta, Mo and W) we have used the 4 parameter modified Morse potential in the NNN approximation. Our potential parameters are taken from Table I of Macdonald and Shukla (MS) (1985) and are listed in Table V. These were derived by MS using the same method outlined in MSK.

All of the values of lattice constant used in our calculations of MSD for the bcc transition metals are taken from room-temperature experimental values of the lattice constant (Pearson 1967) and recommended values of thermal linear expansion (Touloukian 1975).

### 3.4.2 Results and Discussion

We have calculated the MSD of Nb for a number of temperatures in the range 100 K to 500 K. Although thermal expansion data is available for temperatures above 500 K, for Nb only room-temperature experimental values of MSD are available and therefore we have confined our reported results to a low range of temperature in order to clarify the comparison between these results and the experimental data. For the same purpose, our

Table V. Next Nearest Neighbour Potential

Parameters for the bcc transition metals

| | $r_0$ $(\mathring{A})$ | $\alpha$ $(\mathring{A}^{-1})$ | $\epsilon$ $(10^{-12}erg)$ | $b^2$ |
|---|---|---|---|---|
| V | 2.7479 | 0.8963 | 1.2483 | 1.20 |
| Nb | 3.0090 | 0.7530 | 1.7582 | 1.35 |
| Ta | 2.9790 | 1.0294 | 1.9367 | 1.80 |
| Mo | 2.8209 | 1.5135 | 1.6891 | 1.20 |
| W | 2.8331 | 1.5568 | 2.1909 | 1.35 |

From Macdonald and Shukla (1985). The 4 parameter modified Morse potential has been used for all five bcc transition metals.

reported results for the MSD of W and Mo have been confined to a range of temperature for which the comparison with experiment is clearly visible on their respective graphs.

For Nb (Fig. 3.4.1) our QH values of MSD are lower than the $\lambda^2$ PT and RE results at all temperatures. At RT the $\lambda^2$ anharmonic contribution to MSD is positive but very small. The RE values of MSD are larger than the $\lambda^2$ PT results at all temperatures. (This is also true in the cases of V, W, Mo and Ta.) Our results are compared with the experimental data of Bashir et al. (1987). The agreement between theory and experiment is actually worsened by the inclusion of the anharmonic contributions to MSD; however, these are very small and in addition all three of our MSD curves lie almost within the margin of error of the experimental point. The meaningfulness of this result is therefore questionable.

In the case of V (Fig. 3.4.2) no experimental values of MSD could be located for comparison with our results. The anharmonic contribution to MSD is very small below $T_m/4$ but becomes larger with increased temperature until, near $T_m$, the $\lambda^2$ PT and RE values of MSD are 5.6% and 6.5% higher than the QH result respectively.

For W, Mo and Ta the $\lambda^2$ anharmonic contribution to MSD is negative.

Figure 3.4.1.

Comparison of Theory with Experiment for
the Mean Square Displacement of Niobium

The solid lines are the QH, $\lambda^2$ PT and
RE results calculated from the modified Morse
potential. The point represents the experimental
datum of Bashir et al. (1987). D denotes the Debye
temperature. The melting temperature of Niobium
is 2750 K.

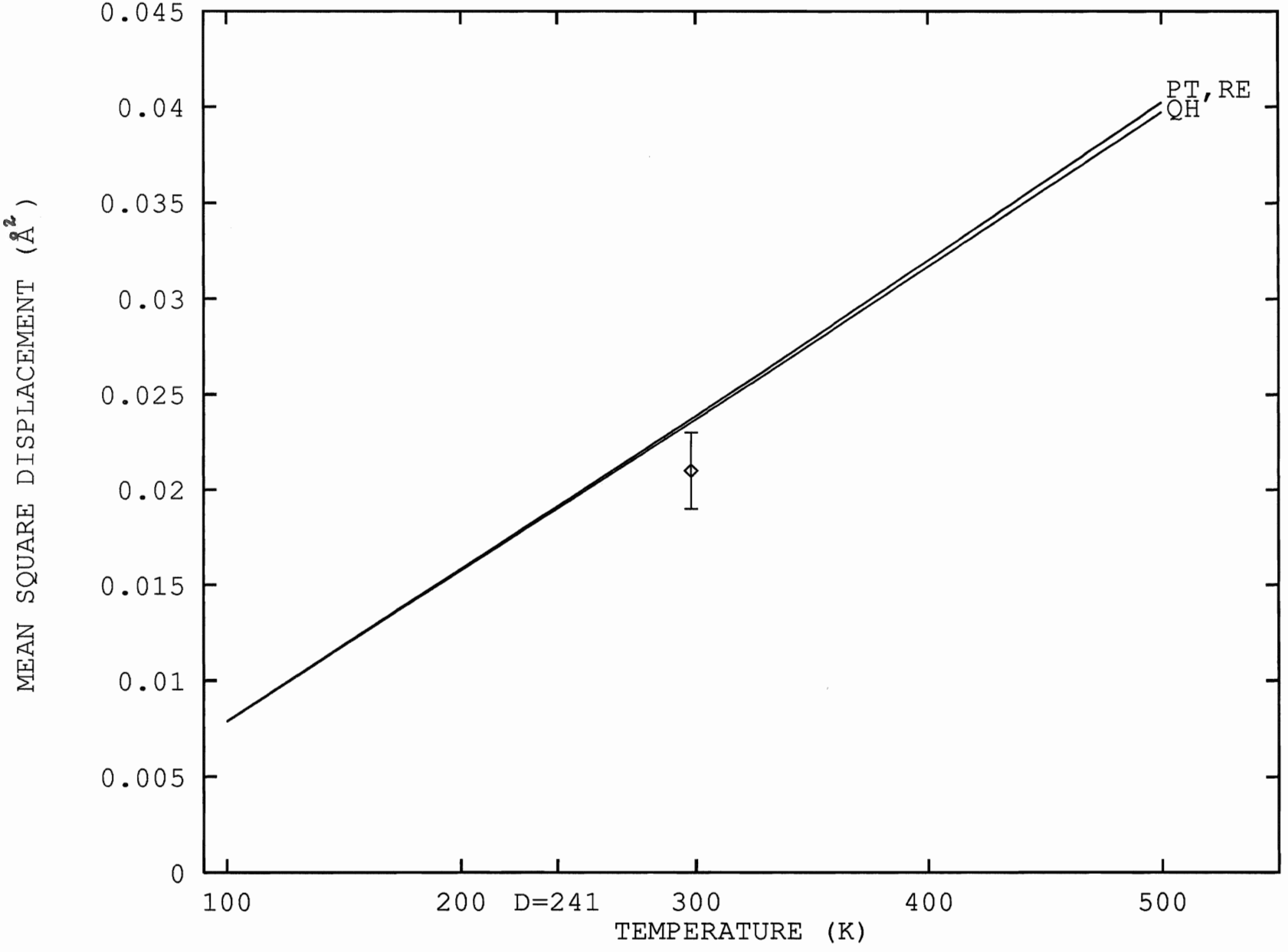
0.045
0.04
0.035
0.03
0.025
0.02
0.015
0.01
0.005
0
MEAN SQUARE DISPLACEMENT (Å²)
PT, RE
QH
100
200
D=241
300
400
500
TEMPERATURE (K)

Figure 3.4.2.

Results for the Mean Square

Displacement of Vanadium

The solid lines are the QH, $\lambda^2$ PT and

RE results calculated from the modified Morse

potential. D denotes the Debye temperature and

M the melting temperature.

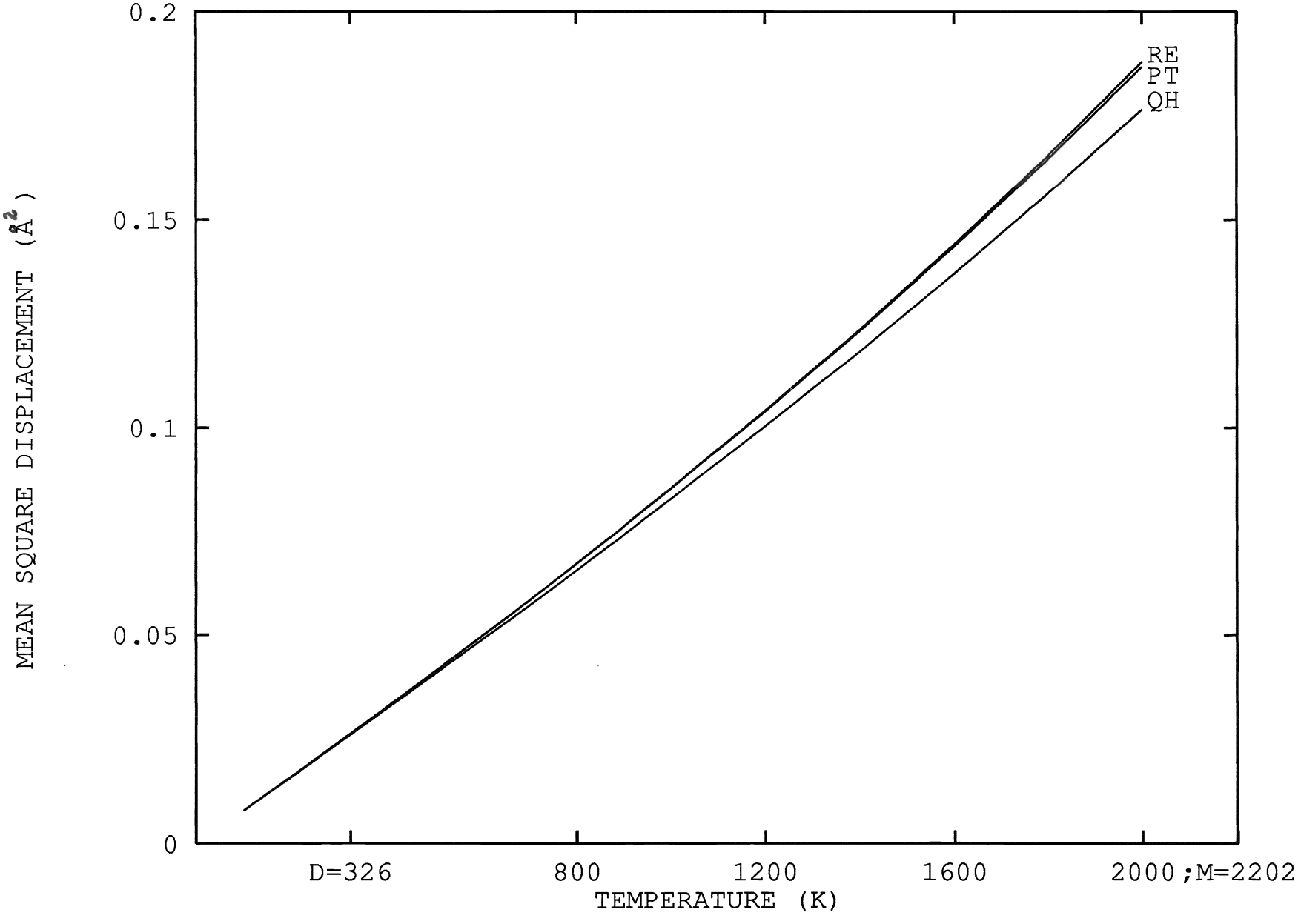
0.2
0.15
0.1
0.05
0
MEAN SQUARE DISPLACEMENT (Å²)
RE
PT
QH
D=326
800
1200
1600
2000;M=2202
TEMPERATURE (K)

In the case of W (Fig. 3.4.3) our results have been compared with the experimental data of Bullard et al.(1991) which were obtained for $^{183}$W at several temperatures in the range 80 K to 1067 K. (It should be pointed out that the experimental values of thermal expansion which we have used in our calculations are for bulk W rather than $^{183}$W.) The anharmonic contribution to MSD clearly improves the agreement between the calculated and experimental results. At 1067 K the QH value of MSD obtained from the modified Morse potential is 13% larger than the experimental data but the $\lambda^2$ PT and RE results are only 7% and 8% larger than the experiment respectively.

In the case of Mo (Fig. 3.4.4), the $\lambda^2$ PT curve is in the best agreement with the RT experimental data of Paakaari (1974). Here the RE curve is practically indistinguishable from the $\lambda^2$ PT curve which indicates that at RT the anharmonic contribution to MSD is adequately represented by the $\lambda^2$ contribution. In the case of Ta (Fig. 3.4.5) the anharmonic contribution to MSD is not very large at any temperature. For Ta no experimental values of MSD could be located for comparison with our results.

For all five of the bcc transition metals for which we have performed calculations of MSD, near RT the anharmonic contribution to MSD is very small and the difference between the $\lambda^2$ PT and RE anharmonic curves is negligible.

Figure 3.4.3.

Comparison of Theory with Experiment for the Mean Square Displacement of Tungsten

The solid lines are the QH, $\lambda^2$ PT and RE results calculated from the modified Morse potential. The points represents the experimental datum of Bullard et al. (1991) D denotes the Debye temperature. The melting temperature of Tungsten is 3695 K.

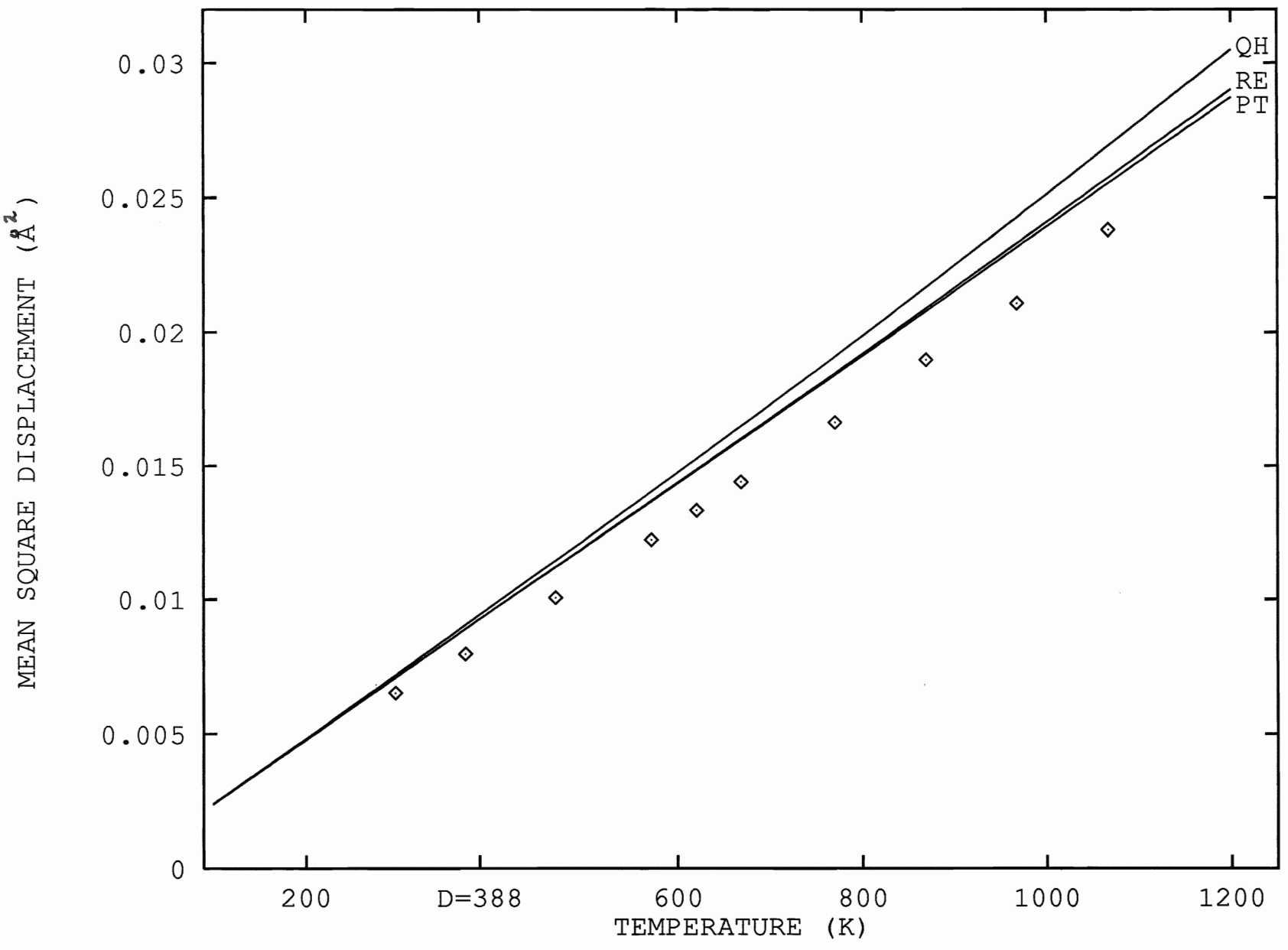
MEAN SQUARE DISPLACEMENT (Å²)
0.03
0.025
0.02
0.015
0.01
0.005
0
200
D=388
600
800
1000
1200
TEMPERATURE (K)
QH
RE
PT

Figure 3.4.4.

Comparison of Theory with Experiment for

the Mean Square Displacement of Molybdenum

The solid lines are the QH, $\lambda^2$ PT and RE results calculated from the modified Morse potential. The point represents the experimental datum of Paakaari (1974). D denotes the Debye temperature. The melting temperature of Molybdenum is 2895 K.

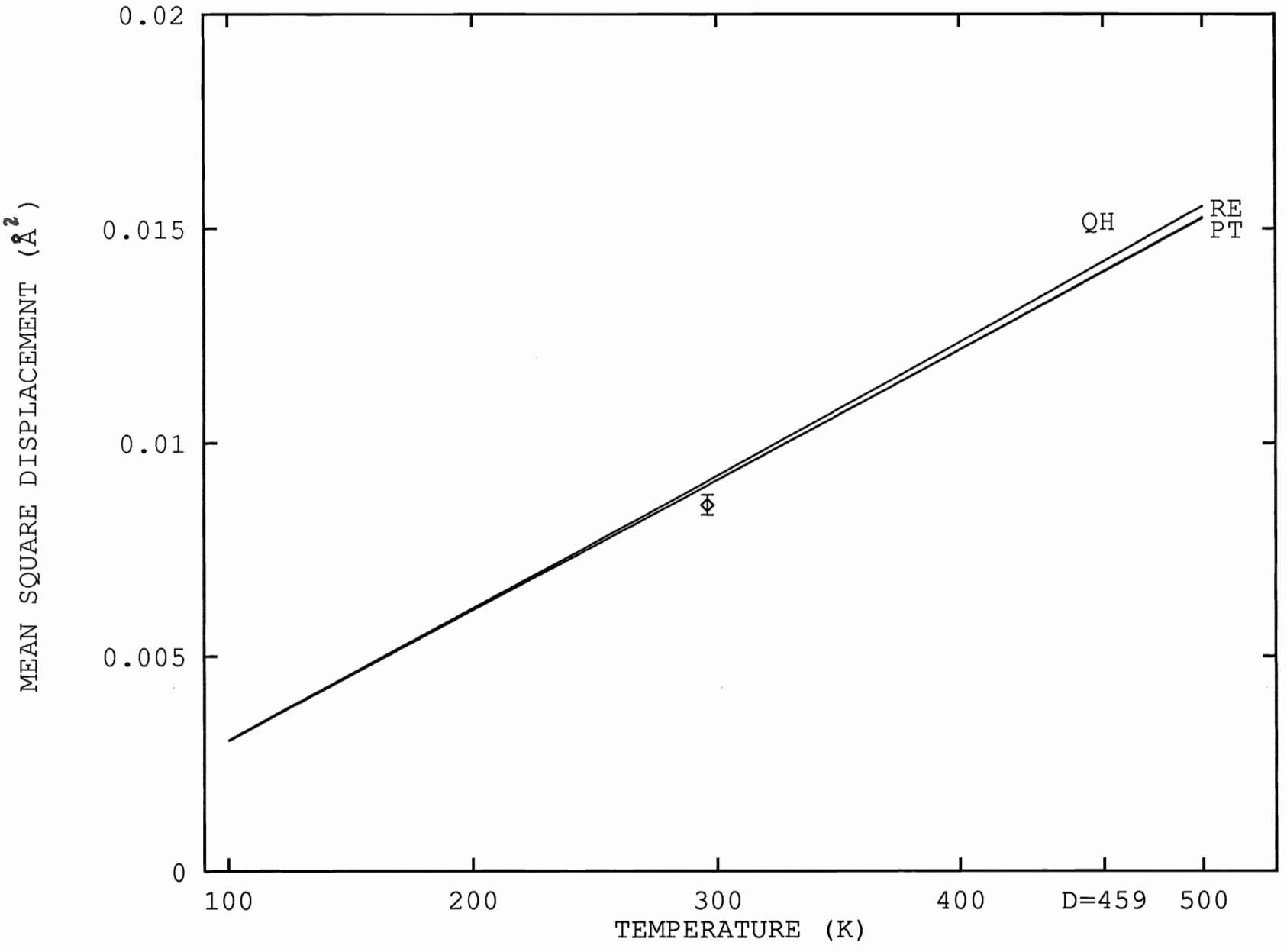
0.02
0.015
0.01
0.005
0
MEAN SQUARE DISPLACEMENT (Å²)
QH
RE
PT
100
200
300
400
D=459
500
TEMPERATURE (K)

Figure 3.4.5.

Results for the Mean Square

Displacement of Tantalum

The solid lines are the QH, $\lambda^2$ PT and

RE results calculated from the modified Morse

potential. D denotes the Debye temperature and

M the melting temperature.

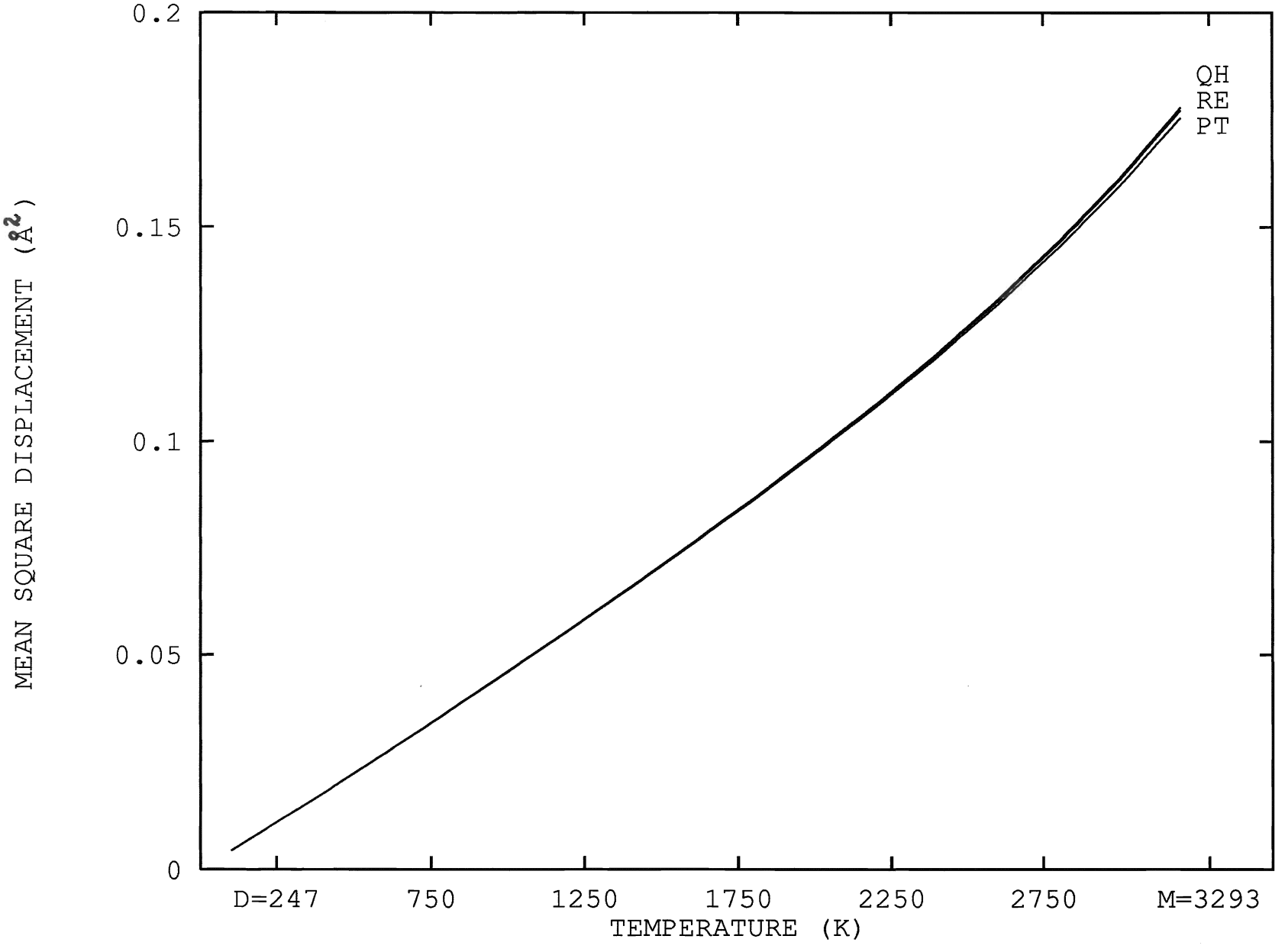
0.2
0.15
0.1
0.05
0
MEAN SQUARE DISPLACEMENT (Å²)
QH
RE
PT
D=247
750
1250
1750
2250
2750
M=3293
TEMPERATURE (K)

The anharmonicity is much larger near the melting point of each solid (with the exception of Ta) but experimental values of MSD are not available for these very large values of $T$. For W the experimental data is available up to about 30% of $T_m$ and in this temperature range the anharmonic contribution to MSD improves the agreement between theory and experiment with the agreement being best for the $\lambda^2$ PT results. For the other four bcc transition metals the quantitative effect of the anharmonic contribution to MSD upon the agreement between theory and experiment is difficult to evaluate due to the sparseness of the experimental data.

# 4. Phonon Dispersion Curves

In order to determine whether the cubic and quartic anharmonic phonon frequency shifts which are obtained from the Green's function method improve the agreement between theoretical and experimental phonon dispersion curves of solids, we have calculated the PDC's of a bcc solid (Na) and an fcc solid (Cu). These calculations have been carried out in the QH approximation and using the Green's function method. In both cases we have used the 4 parameter modified Morse potential. The potential parameters are the same as those used in our calculation of MSD.

The PDC's are a graphical representation of the frequencies of phonon modes whose wavevectors lie in one of the three principal symmetry directions of a cubic solid, ($\zeta$ 0 0), ($\zeta$ $\zeta$ 0), and ($\zeta$ $\zeta$ $\zeta$) where the units of $\zeta$ are the same as those of $p_x, p_y, p_z$ in Chapter 2. In each symmetry direction there are one longitudinal (LO) and two transverse (denoted TR if equal, or TR1 and TR2 if unequal) frequency branches. Since the anharmonic phonon frequency shifts are largest near $T_m$, we have performed our calculations at the highest temperatures for which experimental data is available for comparison with our results.

## 4.1. Phonon Dispersion Curves for Na

The phonon dispersion curves of Na have been experimentally determined at room temperature. A collection of this data, both published and unpublished, appears in Glyde and Taylor (1972). Millington and Squires (1971) have also presented results of their own neutron scattering experiment. In Fig. (4.1.1) we have compared their data with the results of our Morse potential calculations. Our room-temperature lattice constant is taken from Pearson (1967). A step length of 20 was used in the calculation of the $S_{\alpha\beta}$ tensors. In the ($\zeta$ $\zeta$ $\zeta$) symmetry direction the phonon wavevectors for which $\zeta > 0.5$ are outside the first Brillouin zone of the bcc lattice and are therefore not used in the calculation of MSD.

The PDC's of Na which we have calculated in the QH approximation are not in very good agreement with experimental values of phonon frequency. Most of our results are too low. The ($\zeta$ $\zeta$ 0)TR2 and ($\zeta$ $\zeta$ $\zeta$)LO branches are exceptions. In the first of these two cases, all our values of phonon frequency are too high. In the second case, this is only true for some wavevectors outside the FBZ (which are not included in the calculation of MSD).

In general the inclusion of the anharmonic phonon frequency shifts wors-

ens the agreement between theory and experiment for wavevectors lying just inside the BZ boundary [the exception being the ($\zeta$ $\zeta$ 0)LO branch]. This is surprising in light of our results for the MSD of Na in which the RE values of MSD were found to be in better agreement with experiment than the QH values. Since the MSD is calculated from the phonon frequencies, renormalization should produce similar effects upon the agreement between theory and experiment for both the MSD and PDC's if the lattice dynamical model is an accurate representation of the crystal.

This apparent contradiction is at least partially resolved when one realizes that the contributions to MSD arising from individual phonon modes are heavily weighted towards the modes whose wavevectors lie within the central portion of the FBZ, where the values of phonon frequency are relatively small. The effect of anharmonicity upon these phonon frequencies, and the agreement between their values and the experimental data, is difficult to discern in Fig.(4.1.1) so for the purpose of clarity we have enlarged the phonon curves in the ($\zeta$ 0 0) direction in the range $0 \leq \zeta \leq 0.25$. This enlargement is presented in Fig.(4.1.2). Fig.(4.1.2) shows that four of the five experimental points which lie in this range are in better agreement with the RE phonon curves than the QH curves. Near the zone boundary the

QH curve is of course in better agreement with experiment but these phonon frequencies do not make much of a contribution to the MSD. This is also the case in the ($\zeta$ $\zeta$ $\zeta$)TR phonon branch where the RE curve is closer to the experimental data at low $\zeta$ while near the zone boundary the QH curve is in the best agreement with experiment.

The modified Morse potential does not predict the PDC's of Na with much accuracy and the RE results are, in general, in worse agreement with experiment than the QH results, particularly near the zone boundary. However, a closer examination of the phonon dispersion curves reveals that this latter conclusion does not necessarily contradict the results which we have already obtained for the MSD of Na.

Figure 4.1.1.

Comparison of Theory with Experiment for
the Phonon Dispersion Curves of Sodium

The solid and dashed lines are the QH and RE
results from the modified Morse potential.
The points represent room-temperature experimental
data tabulated in Glyde and Taylor (1972) and
and the crosses represent the experimental data
of Millington and Squires (1971). LO and TR
denote longitudinal and transverse branches
respectively.

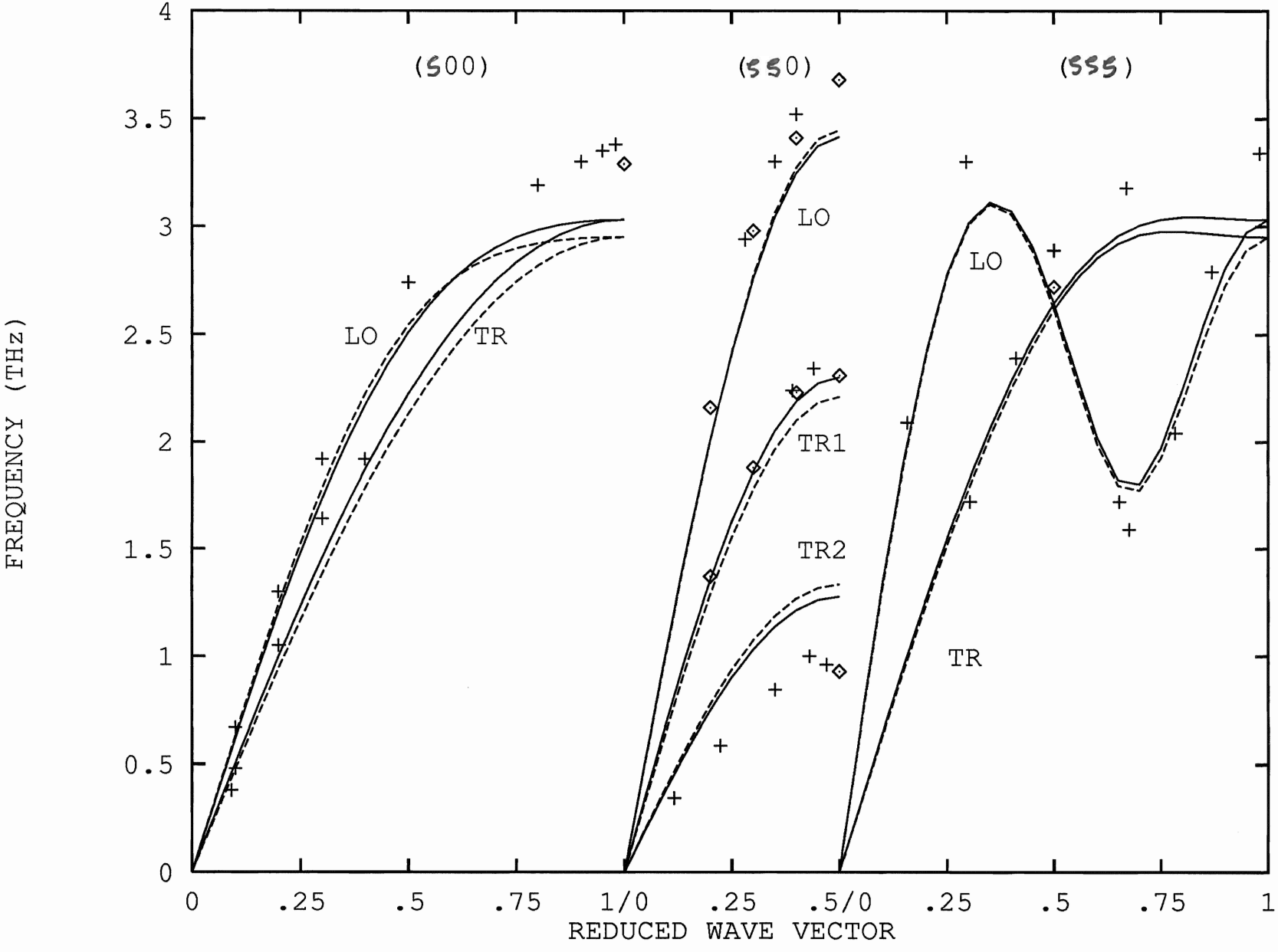
(S00)
(S50)
(S55)
LO
TR
LO
TR1
TR2
LO
TR
FREQUENCY (THz)
REDUCED WAVE VECTOR
0
.25
.5
.75
1/0
.25
.5/0
.25
.5
.75
1
0
0.5
1
1.5
2
2.5
3
3.5
4

Figure 4.1.2.

Comparison of Theory with Experiment for the

($\zeta$ 0 0) Phonon Dispersion Curves of Sodium:

Enlarged View in the Long-Wavelength Region

The legend is the same as that of Fig.(4.1.1).

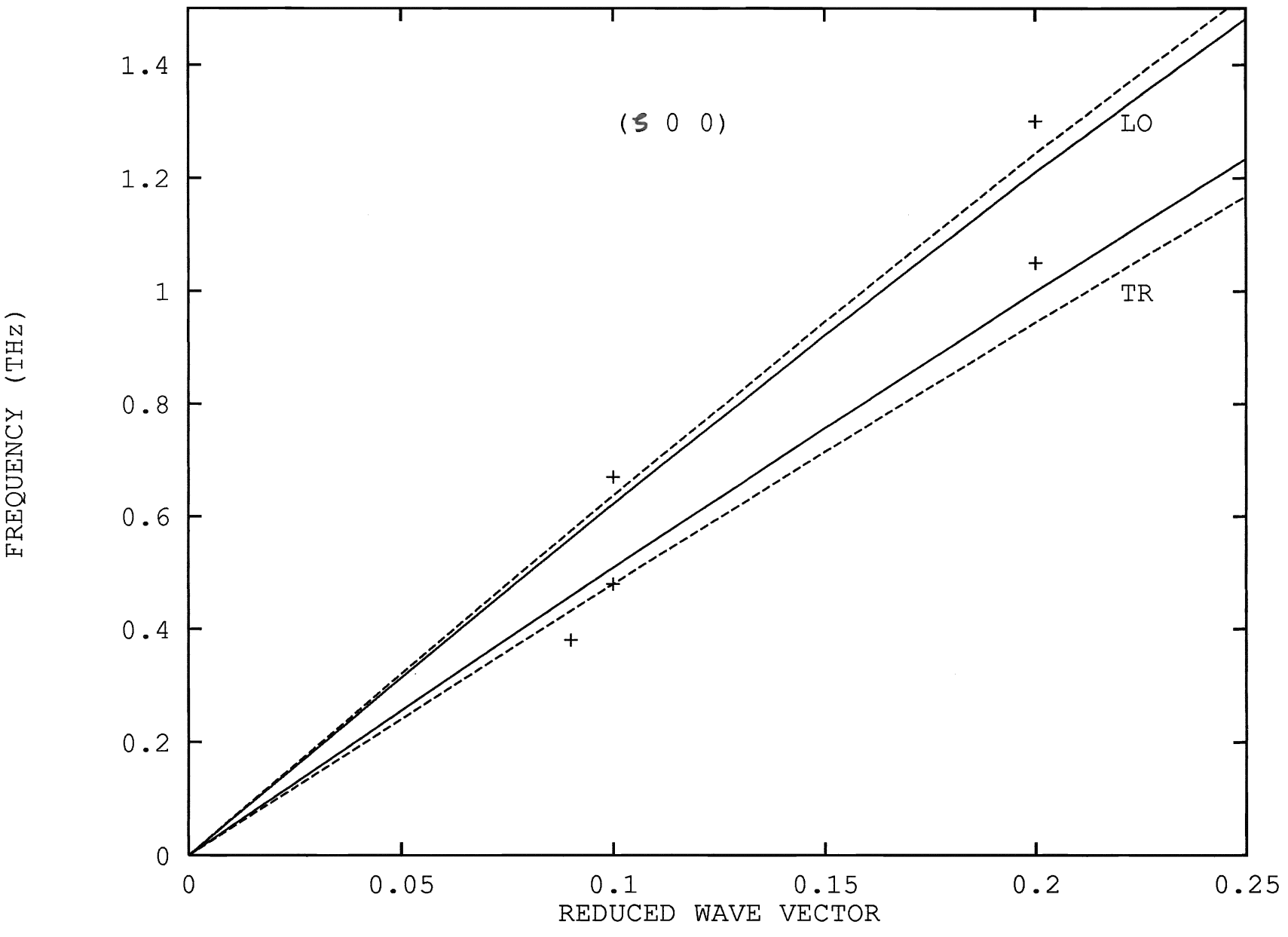
(ξ 0 0)
LO
TR
FREQUENCY (THz)
REDUCED WAVE VECTOR
0
0.2
0.4
0.6
0.8
1
1.2
1.4
0
0.05
0.1
0.15
0.2
0.25

## 4.2. Phonon Dispersion Curves for Cu

Larose and Brockhouse (1976) (LB) have measured the PDC's of Cu in the ($\zeta$ 0 0) and ($\zeta$ $\zeta$ 0) principal symmetry directions at 1336 K. Although their values of phonon frequency have only been presented in the form of a graph, they have provided the force constants of a five-neighbour Born-von Karman fit which we have used to reproduce the experimental PDC's and to obtain the PDC's in the ($\zeta$ $\zeta$ $\zeta$) symmetry direction. We have also used their value of the 1336 K lattice constant (3.6928 $\mathring{A}$). A step length of $L = 20$ was used in the calculation of the $S_{\alpha\beta}$ tensors. For the fcc lattice, the wavevectors in the ($\zeta$ $\zeta$ 0) symmetry direction for which $\zeta > \frac{1}{\sqrt{2}}$ lie outside the FBZ and therefore they are not involved in the calculation of MSD.

Our results are presented in Figure (4.2.1) along with the experimental data of LB. Our QH phonon curves are in poor agreement with experiment. However, wherever the QH and RE curves can be visually distinguished the inclusion of the anharmonic phonon frequency shifts improves the agreement between theory and experiment for all the phonon branches in the principal symmetry directions, with the improvement being most marked in the ($\zeta$ 0 0)L and ($\zeta$ $\zeta$ 0)T1 phonon branches.

As in the case of Na we also want to examine the effect of renormalization upon the low-frequency phonon modes. Since this effect is difficult to discern in Fig.(4.2.1) we have enlarged the long-wavelength regions of all the dispersion curves. Fig.(4.2.2) is an enlargement of the dispersion curves in the ($\zeta$ 0 0) direction and Fig.(4.2.3) is a similar enlargement of the dispersion curves in the ($\zeta$ $\zeta$ 0) and ($\zeta$ $\zeta$ $\zeta$) directions. In both these graphs the values of $\zeta$ are restricted to the range $0 \leq \zeta \leq 0.25$.

Figs.(4.2.2) and (4.2.3) show that, in the case of the transverse phonon branches, the RE phonon curves are in the best agreement with the experiment in all three symmetry directions and at all values of $\zeta$. For the longitudinal branches, however, the QH curves are in better agreement with the Born-von Karman fit at the lowest values of $\zeta$. However, here the anharmonic frequency shifts are extremely small, and these only become appreciable at larger values of $\zeta$ for which the RE curves are actually in the best agreement with the experiment. These results are consistent with our results for the MSD of Cu in which the renormalized values of MSD agreed better with experiment than the QH values. In all three longitudinal branches the QH and RE curves cross between $\zeta = 0.1$ and $\zeta = 0.25$.

The modified Morse potential is much more successful in predicting the

phonon dispersion curves for Cu than for Na, in both the QH approximation and using the Green's function method.

Figure 4.2.1.

Comparison of Theory with Experiment for the Phonon Dispersion Curves of Copper

The solid and dashed lines are the QH and RE results from the modified Morse potential. The points represent experimental values of phonon frequency reproduced from the Born-von Karman fit of Larose and Brockhouse (1976). LO and TR denote longitudinal and transverse phonon branches respectively.

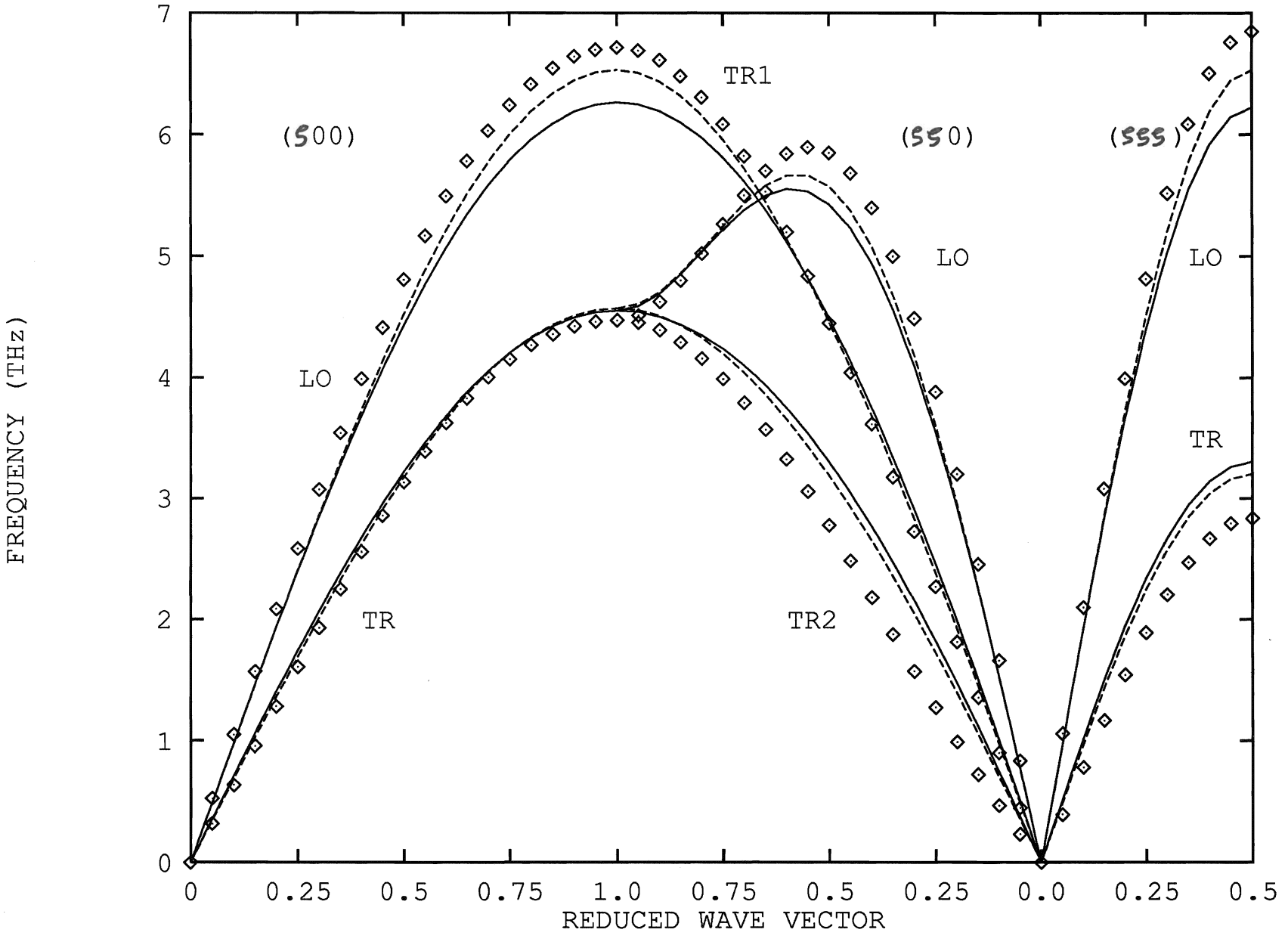
FREQUENCY (THz)
7
6
5
4
3
2
1
0
(500)
(550)
(555)
TR1
LO
LO
LO
TR
TR
TR2
0
0.25
0.5
0.75
1.0
0.75
0.5
0.25
0.0
0.25
0.5
REDUCED WAVE VECTOR

Figure 4.2.2.

Comparison of Theory with Experiment for the

($\zeta$ 0 0) Phonon Dispersion Curves of Copper:

Enlarged View in the Long-Wavelength Region

The legend is the same as that of Fig.(4.2.1).

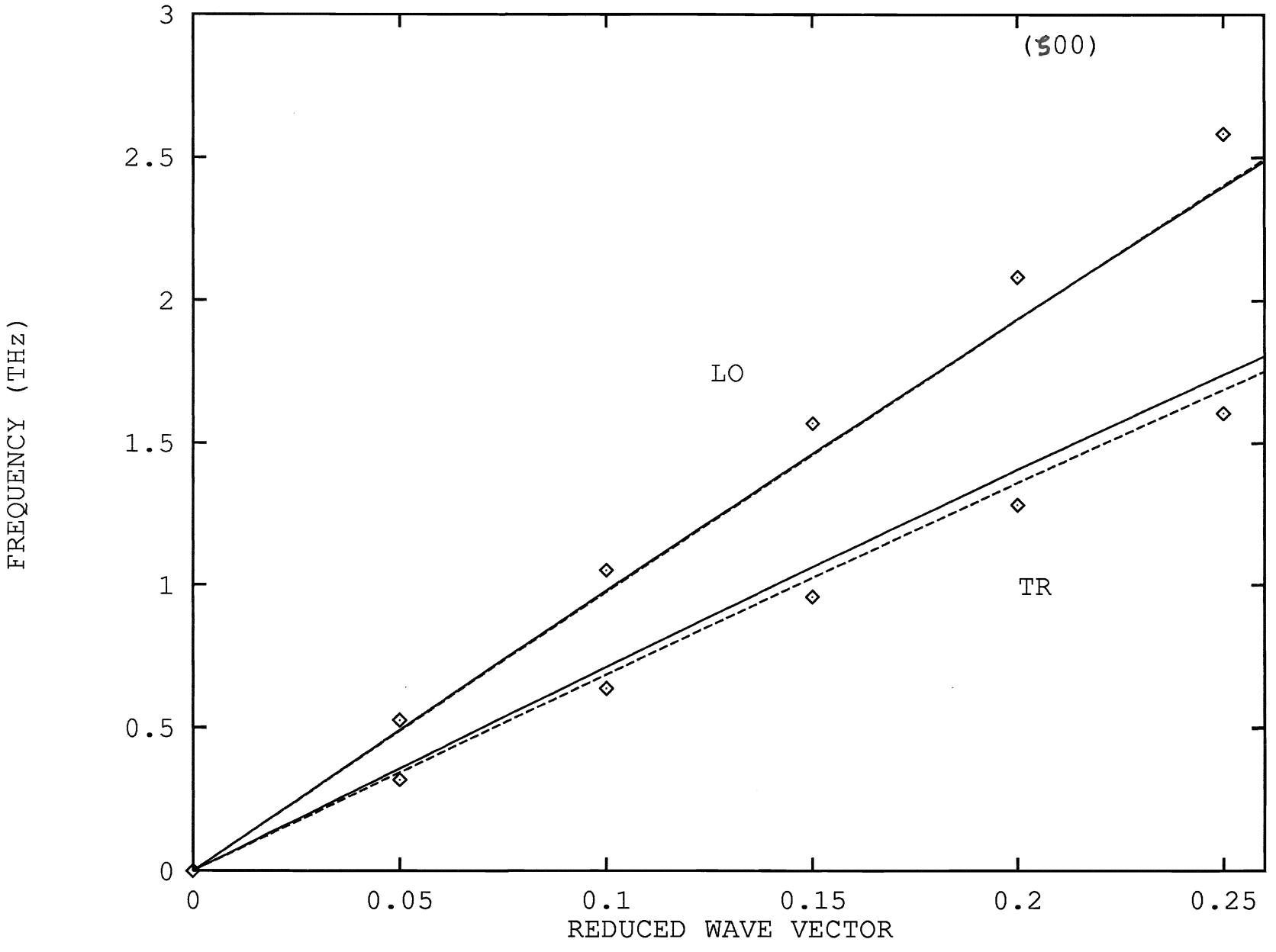
(500)
LO
TR
FREQUENCY (THz)
REDUCED WAVE VECTOR
0
0.5
1
1.5
2
2.5
3
0
0.05
0.1
0.15
0.2
0.25

Figure 4.2.3.

Comparison of Theory with Experiment for the

$(\zeta\ \zeta\ 0)$ and $(\zeta\ \zeta\ \zeta)$ Phonon Dispersion Curves

of Copper: Enlarged View in the Long-Wavelength Region

The legend is the same as that of Fig.(4.2.1)

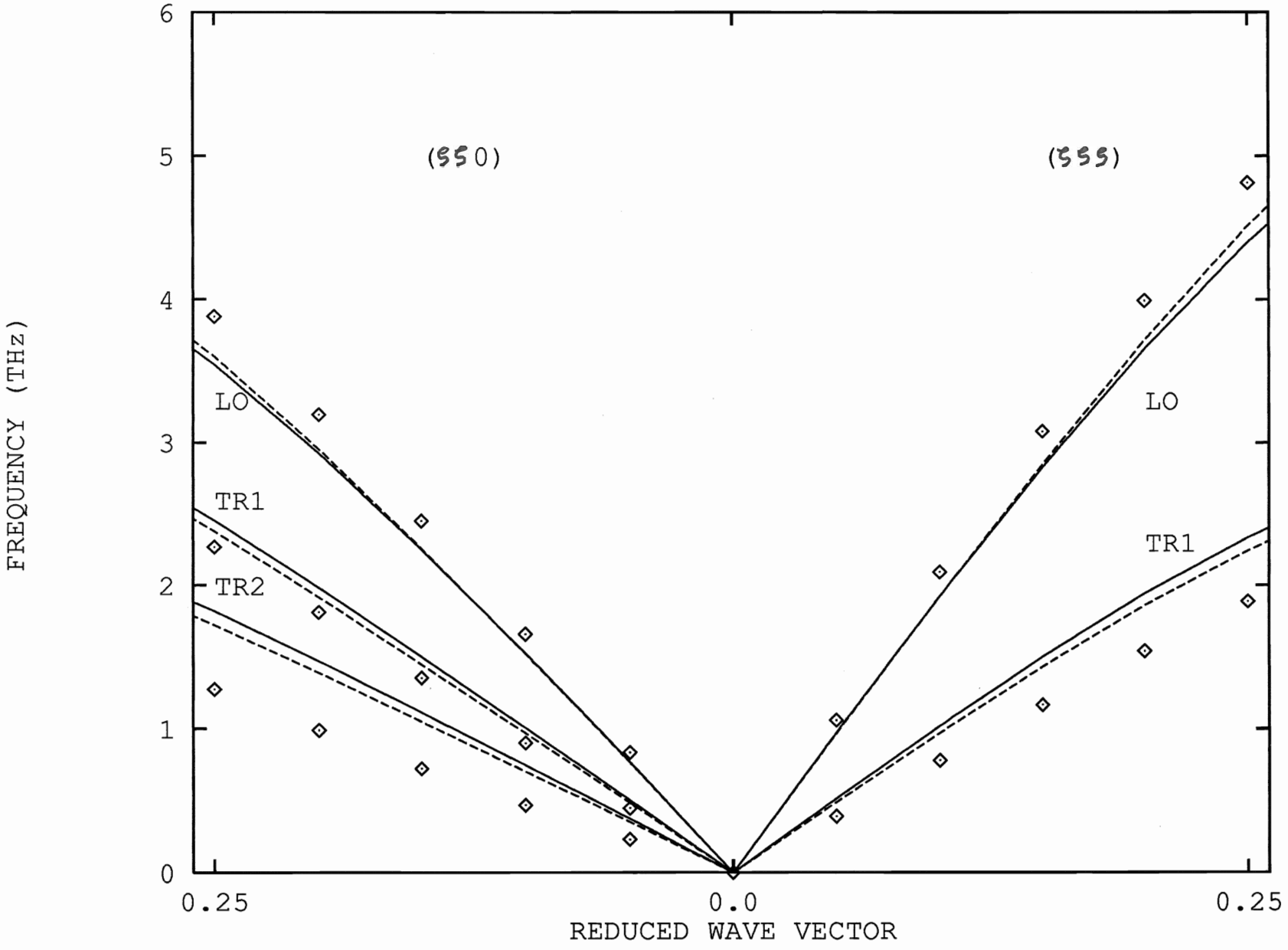
6
5
4
3
2
1
0
(550)
(555)
LO
TR1
TR2
LO
TR1
FREQUENCY (THz)
0.25
0.0
0.25
REDUCED WAVE VECTOR

# 5. Summary

We have calculated the MSD of a central-force Lennard-Jones solid in the nearest-neighbour (NN) and next-nearest neighbour (NNN) approximations and have applied our results to a solid for which the L-J potential is appropriate (Xe) in order to determine the effect of the range of the interatomic interaction on the MSD. In the QH approximation the NN and NNN results for MSD only differ by about 2% at the highest temperatures. However, when the anharmonic contribution to MSD is included (this is the case in the $\lambda^2$ and Green's function methods), the agreement between the NN and NNN results worsens. We conclude that the second neighbour interactions are important in the anharmonic calculation of MSD of a Lennard-Jones solid but are not so important in the QH case. Comparison of our $\lambda^2$ results for MSD of Xe with the $\lambda^2$ results of Goldman show that the frequency-shift approximation used by Goldman is not a very good approximation.

We have performed lattice-dynamics calculations of the atomic mean-square displacement (MSD) of a number of fcc and bcc metals using the 3 parameter Morse potential, the 4 parameter modified Morse potential and (for Cs alone) the 3 parameter Rydberg potential. These calculations have

been carried out in the QH approximation and also using PT of lowest order and the Green's function method (RE). For the fcc metals we have used the NN approximation but for the bcc metals the NNN approximation has been used.

For most of the materials for which experimental data is available for comparison with our results, the RE values of MSD are in the best agreement with experiment. However, in general the RE results are not in much better agreement with experiment than the $\lambda^2$ PT and QH results. For the Morse potential, the improvement in the agreement between theory and experiment which the anharmonic contribution to MSD produces is mostly qualitative.

We have also calculated the phonon dispersion curves (PDC's) of Na and Cu using the QH theory and the Green's function method. The interatomic potential used in these calculations is the 4 parameter modified Morse potential. For Na our calculated PDC's are in poor agreement with experiment. For Cu the agreement between theory and experiment is poor for the QH results but for the RE results the anharmonic frequency shift produces excellent quantitative improvement in this agreement.

# References


J.Bashir, Q.H.Khan, and N.M.Butt, Acta.Cryst.A**43**, 795 (1987)

B.Bednarz and D.W.Field, Acta.Cryst.A**38**, 3 (1982a)

B.Bednarz and D.W.Field, Acta.Cryst.A**38**, 163 (1982b)

B.N.Brockhouse and A.T.Stewart, Phys.Rev.**100**, 756 (1955)

J.S.Brown, Proc.Phys.Soc.**85**, 394 (1965)

B.R.Bullard, J.G.Mullen and G.Schupp, Phys.Rev.B**43**, 7405 (1991)

J.R.D.Copley and B.N.Brockhouse, Can.J.Phys.**51**, 2564 (1973)

J.R.D.Copley, C.A.Rotter, H.G.Smith, and W.A.Kamitakahara, Phys.Rev.Lett.**33**, 365 (1974)

D.Cribier, B.Jacrot and D.Saint-James, in *Inelastic Scattering of neutrons in solids and liquids* (I.A.E.A Vienna) p.549 (1961)

M.L.Crow, G.Schupp, W.B.Yelon, J.G.Mullen and A.Djedid, Phys.Rev.B**39**, 909 (1989)

H.R.Glyde and R.Taylor, Phys.Rev.B**5**, 1206 (1972)

V.V.Goldman, Phys.Rev.**174**, 1041 (1968)

O.P.Gupta, J.Phys.Soc.Japan **38**, 1451 (1975)

G.A.Heiser, R.C.Shukla and E.R.Cowley, Phys.Rev.B **33**, 2158 (1986)

H.Hubschle and R.C.Shukla, Phys.Rev.B **40**, 11920 (1989)

E.H.Jacobsen, Phys.Rev.**97**,654 (1955)

H.L.Kharoo, O.P.Gupta, and M.P.Hemkar, J.Phys.Soc.Jpn.**43**,2030 (1977)

R.C.G.Killean, J.Phys.F:Metal Physics **4**, 1908 (1974)

M.L.Klein and J.A.Venables, in *Rare Gas Solids*, vol.II, Academic Press, London (1977)

M.S.Kushwawa, Phys.Stat.Solidi **B96**, 301 (1979)

A.Larose and B.N.Brockhouse, Can.J.Phys.**54**, 1990 (1976)

E.J.Lisher, Acta.Cryst.A**32**, 506 (1976)

R.A.Macdonald and W.M.Macdonald, Phys.Rev.B**24**, 1715 (1981)

R.A.Macdonald and R.C.Shukla, Phys.Rev.B**32**, 4961 (1985)

R.A.Macdonald, R.C.Shukla and D.K.Kahaner, Phys.Rev.B**29**, 6489 (1984)

A.A.Maradudin and P.A.Flinn, Phys.Rev.**129**, 2529 (1963)

C.J.Martin and D.A.O'Connor, Acta.Cryst.A**34**, 500 (1978)

M.Merisalo, M.S.Lehmann, and F.K.Larsen, Acta.Cryst.A**40**, 127 (1984)

A.P.Miller and B.N.Brockhouse, Can.J.Phys **49**, 704 (1971)

A.J.Millington and G.L.Squires, J.Phys.F:Metal Physics **1**, 244 (1971)

R.M.Nicklow, G.Gilat, H.G.Smith, L.J.Raubenheimer and M.K.Wilkinson, Phys.Rev.**164**, 922 (1967)

Ph.Olmer, Acta.Cryst.**1**, 57 (1948)

T.Paakkari, Acta.Cryst.A**30**, 83 (1974)

S.Pal, Can.J.Phys.**51**, 1869 (1973)

W.B.Pearson, *A Handbook of Lattice Spacings and Structures of Metals and Alloys* (Pergamon, Oxford, 1967) vol.2

J.Prakash and M.P.Hemkar, J.Phys.Soc.Japan **34**, 1583 (1973)

J.Prakash, L.P.Pathak and M.P.Hemkar, Aust.J.Phys **28**, 63 (1975)

A.Rosengren and B.Johansson, J.Phys.F:Metal Physics **5**, 629 (1975)

S.K.Sanga, P.K.Sharma, Z.Phys.Chemie **247**, 257 (1971)

R.C.Shukla, J.Chem.Phys.**45**, 4178 (1966)

R.C.Shukla, Int.J.Thermophys.**1**, 73 (1980)

R.C.Shukla, Phys.Rev.B**23**, 3087 (1981)

R.C.Shukla, Phil.Mag.Letters, **70**, 255 (1994)

R.C.Shukla and G.A.Heiser, Phys.Rev.B **33**, 2152 (1986)

R.C.Shukla and H.Hubschle, Phys.Rev.B **40**, 1555 (1989a)

R.C.Shukla and H.Hubschle, Sol.State Comm. **72**, 1135 (1989b)

R.C.Shukla and R.D.Mountain, Phys.Rev.B **25**, 3649 (1982)

R.C.Shukla and E.R.Muller, Phys.Stat.Sol.B **43**, 413 (1971)

R.C.Shukla and C.A.Plint, Phys.Rev.B **40**, 10337 (1989)

R.C.Shukla and F.Shanes, Phys.Rev.B **32**, 2513 (1985)

R.C.Shukla and L.Wilk, Phys.Rev.B **10**, 3660 (1974)

M.Simerska, Acta.Crst.A**14**, 1259 (1961)

N.Singh and P.K.Sharma, Phys.Rev.B **3**, 1141 (1971)

S.K.Sinha, Phys.Rev.**143**, 422 (1966)

E.C.Svensson, B.N.Brockhouse and J.M.Rowe, Phys.Rev.**155**, 619 (1967)

Y.S.Touloukian, R.K.Kirby, R.E.Taylor, and P.D.Desai, *Thermal Expansion, Metallic Elements and Alloys*, Vol.12 of the *TPRC Series on Thermophysical Properties of Matter*, ed. Y.S.Touloukian and C.Y.Ho (Plenum, New York, 1975)

B.B.Tripathi and J.Behari, J.Phys.F:Metal Physics **1**, 19 (1971)

A.D.B.Woods, B.N.Brockhouse, R.H.March and R.Bowers, Proc.Phys.Soc. **79**, 440 (1962)

D.N.Zubarev, Soviet Phys. - Uspekhi **3**, 320 (1960)